Journal of Environmental Chemical Engineering 10 (2022) 108955

Contents lists available at ScienceDirect

Journal of Environmental Chemical Engineering

journal homepage: www.elsevier.com/locate/jece

Magnetic nanoparticles draw solution for forward osmosis: Current status and future challenges in wastewater treatment

MhdAmmar Hafiz [a], Amani Hassanein [a], Mohammed Talhami [a], Maryam AL-Ejji [b], Mohammad K. Hassan [b], Alaa H. Hawari [a,*]

[a] Department of Civil and Architectural Engineering, College of Engineering, Qatar University, PO Box 2713, Doha, Qatar
[b] Center of Advanced Materials, Qatar University, PO Box 2713, Doha, Qatar

ARTICLE INFO

Keywords:
Forward osmosis
Draw solution
Magnetic nanoparticles
Magnetite surface modification
Wastewater treatment

ABSTRACT

Forward osmosis is considered as the least energy intensive membrane process since it operates based on the osmotic pressure gradient. However, it is still considered as immature technology mainly due to the elevated cost for draw solution regeneration. Nevertheless, magnetic nanoparticles could be considered as a sustainable draw solute for forward osmosis due to high osmotic pressure and easy regeneration using magnetic force, but a significant development is still needed before implementing it for wastewater treatment and desalination. Herein, we analyzed the performance of the available magnetic nanoparticles draw solute and identified the challenges facing the use of magnetic nanoparticles as draw solute in the forward osmosis process. We first highlight the common synthesis methods of magnetic nanoparticles, and basics for generation of osmotic pressure using magnetic nanoparticles. Then, we analyzed the performance and limitations of available magnetic nanoparticles that were used as draw solute in the forward osmosis process. Later, we assessed the toxicity level of the magnetic nanoparticles and explored the regulations of using magnetic nanoparticles in the water treatment industry. Finally, new avenues of research were proposed to make magnetic nanoparticles draw solution more effective when applying it in desalination and wastewater treatment process.

1. Introduction

Membrane processes are promising technology for desalination and wastewater treatment. Currently, reverse osmosis is the most commonly used membrane process, but high energy consumption [1] and membrane fouling [2,3] are considered as major draw backs for the technology. Forward osmosis (FO) is considered as the least energy intensive membrane process since it operates based on the osmotic pressure gradient [4]. The osmotic pressure gradient is generated between low salinity feed solution (FS) and high salinity draw solution (DS), separated by a semipermeable membrane [5]. Also, FO can resist membrane fouling caused by a feed water contaminated with organic, biological and particulate matter [6]. Although FO has low energy consumption and high resistance to fouling, it is still considered as immature technology mainly due to elevated cost for DS regeneration [7]. Draw solution regeneration is a process used to recover the draw solute from the diluted draw solution after the FO process to make the product water suitable for the final application. The currently used draw solutes are regenerated by energy intensive processes such as reverse osmosis and thermal desalination processes. The energy cost of the regeneration process adds up to the total cost of the water treatment process which negatively affects the economic viability of the FO process. In the last decade, a remarkable progress has been made in developing FO membrane [8–10], but new advances in developing superior DS are considered as a crucial necessity to successfully commercialize the FO process in wastewater treatment and desalination industry.

The main characteristics of a superior DS are as follows 1) high osmotic pressure (high water flux) [11]; 2) low reverse solute flux [12]; 3) easy and efficient recovery from the diluted DS; 4) low toxicity if the permeate will be consumed by humans / animals [7]; 5) inexpensive to make sure that it is feasible for commercialization [13]; 6) hydrophilic nature to assure good interaction with water molecules [14]. A range of draw solutes were tested over the past years including; organic solutes [15–20], inorganic solutes [21–25] and volatile compounds [26,27]. However, the available draw solutes have various limitations such as costly recovery, limited recyclability and reverse diffusion [28].

* Corresponding author.
E-mail address: a.hawari@qu.edu.qa (A.H. Hawari).

https://doi.org/10.1016/j.jece.2022.108955
Received 29 August 2022; Received in revised form 16 October 2022; Accepted 9 November 2022
Available online 11 November 2022

Therefore, the FO process could become economically feasible when the regeneration of DS becomes sustainable and cost effective. Magnetic nanoparticles (MNPs) could be a sustainable draw solute for the FO process due to high osmotic pressure and easy regeneration using magnetic force, but a huge development is still needed before implementing it in the FO process for wastewater treatment and desalination.

FO draw solutes have been reviewed in the literature [28–33], however, none of the studies were focused on magnetic nanoparticles as draw solution. In this review article, we examine the performance and challenges of the available MNPs draw solution to create an efficient MNPs which could be used as draw solute in the FO process. We first highlight the common synthesis methods of MNPs, and the basics for generation of osmotic pressure using MNPs. Then, we study the performance and limitations of the available MNPs that was used as draw solute in the FO process. Afterward, we assess the toxicity level of the MNPs and the regulations of using nanoparticles in water treatment industry. We conclude by proposing new avenues of research to make magnetic nanoparticles draw solution more feasible when applying it in the FO process for desalination and wastewater treatment.

2. Types and synthesis methods of iron oxide magnetic nanoparticles

Magnetic iron oxides nanoparticles are commonly available in three different forms: maghemite (γ-Fe_2O_3), magnetite (Fe_3O_4), and hematite (α-Fe_2O_3). The property of each form of the magnetic iron oxide nanoparticles is distinct, which makes the classifications necessary before being employed in a specific application [34,35]. The structure and physical characteristics of the hematite, magnetite, and maghemite are summarized in Table 1. Their crystal structure is described as a close-packed oxygen anions lattice with smaller iron cations filling the octahedral and tetrahedral interstitial sites. Hematite has O^{2-} anions arranged in a hexagonal closely packed lattice with Fe^{3+} cations in octahedral sites. As for the magnetite and maghemite, O^{2-} anions are arranged in a close-packed cubic structure. Magnetite has an inverse spinel structure with Fe^{3+} cations irregularly distributed between octahedral and tetrahedral sites, and Fe^{2+} cations located in octahedral sites. Maghemite is formed when all Fe oxidizes to Fe^{3+} which has a similar spinel structure to magnetite, however, it has vacancies in the octahedral sublattice. Two-thirds of the sites are occupied by Fe^{3+} cations, which are grouped in a regular pattern, with two occupied sites followed by one unoccupied site. Each form of the magnetic iron oxide nanoparticle has a distinct color, the hematite and maghemite could be formed in two colors, blood-red when finely split, and black or grey when coarsely crystalline. On the other hand, magnetite is black in color irrespective of the form. In terms of stability, hematite is the most stable form of iron oxide at ambient conditions, thus, it is usually the end-product of all iron oxides transformation. With respect to hematite, maghemite is metastable, and it can be formed as a product of iron oxide heating, and with magnetite it forms continuous solid solutions. However, magnetite is not stable under ambient conditions since it can easily oxidize to Fe_2O_3 or dissolve in acidic environments [36]. Magnetite and maghemite, especially magnetite, are the most used forms of the iron oxide nanoparticle owing to the high magnetization, low level of toxicity, and easy synthesis [37,38]. Magnetite nanoparticles has captivated the research interests due to their ability to exhibit high magnetic characteristic, especially when the particles size is reduced so that each particle will have a single domain [34]. In addition, the magnetization of the magnetite nanoparticles occurs up to their magnetic saturation when applying an external magnetic field, however, they do not show any magnetic interaction after the removal of the external magnetic field.

Several methods have been developed for the synthesis of MNPs, categorized as chemical and physical methods. Physical methods include, gas-phase deposition [40], pulsed laser ablation [41,42], electron beam lithography [43], power ball milling [44], laser-induced pyrolysis [45], and combustion [46]. Physical methods are preferred for large-scale production which imply simple processes. Nevertheless,

Table 1
Physical and structural characteristics of the most common forms of the magnetic iron oxide nanoparticles.

Iron oxide	Formula	Color	Crystallographic system	Structural type	Type of magnetism	Magnetic saturation (Am^2/Kg)	Curie temperature transition (K)	Ref
Hematite	α-Fe_2O_3	Grey, black, red	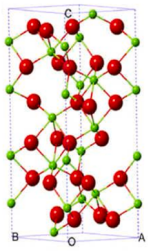	Corundum	Weakly ferromagnetic or antiferromagnetic	0.3	~ 1000	[34,37, 168]
Magnetite	Fe_3O_4	Black	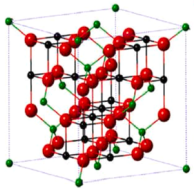	Inverse spinel	Ferromagnetic	92–100	~ 850	[34, 168]
Maghemite	γ-Fe_2O_3	Grey, black, red	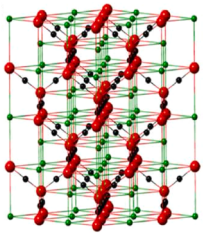	Defect spinel	Ferrimagnetic	60–80	~ 820–986	[34,39, 168]

major limitations occur due to the barely dispersed particle size distribution, costly technologies, and time-consuming process [47]. Chemical methods are based upon the formation of nanoparticles from molecules that contains iron condensate in a certain experimental condition. They can be carried out to synthesize a nano-scaled superparamagnetic particles [34]. Chemical methods include, co-precipitation [48], thermal decomposition [49], hydrothermal synthesis [50], and microemulsions [51]. In the chemical methods, the properties of the MNPs can be controlled easily by adjusting the reaction parameters such as temperature, ionic strength, pH, and type of alkaline. The limitations of the chemical methods are lacking a uniform particle size distribution [34], and the requirement of a strong base in the synthesis process. Mild bases can be used instead of strong bases, however it may result in slower rate of precipitation [47]. In addition, the obtained iron oxide particles from this method are often instable, therefore a stabilizing agent must be used to enhance the stability of the particles [52].

Depending on the application, choosing the appropriate method of preparation is a key factor in producing MNPs with desirable properties. The properties include particles size, shape, surface charge, colloidal stability, and magnetic characteristics. However, chemical methods specifically co-precipitation and thermal decomposition methods stand out as the most convenient approaches in preparing MNPs owing to their inherent simplicity and effectiveness in controlling the composition of nanoparticles [53]. Thermal composition and chemical co-precipitation are also the sole methods used in the preparation of MNPs draw solution used in the FO process [54]. Therefore, this section will be focused on co-precipitation and thermal decomposition methods.

2.1. Chemical co-precipitation

Co-precipitation is defined as the concurrent formation of nucleation, growth, coarsening, and/or agglomeration processes. The process of nucleation is when nuclei (seeds) serve as templates for crystal growth. In the case of homogeneous nucleation, a uniform formation of nuclei throughout the parent phase occurs. While heterogeneous nucleation occurs when it forms based on structural inhomogeneities such as impurities, container surfaces, dislocations, and grain boundaries. In liquid phase synthesis reactions, heterogenous nucleation is the case since a stable nucleating surface already exist [55] which is the case in co-precipitation process [56]. This process occurs under supersaturation condition to urge the precipitation reaction. At the nucleation stage, a large number of crystalline particles are formed and precipitated from a supersaturated solution until the amount of constituent species decreases, which results in the formation of nanoparticle crystals. Nucleation duration is very short while the growth process is a slow-controlled phase that occurs due to the dispersion of solute from the solution on the crystal's surface [57]. Due to Ostwald ripening processes, post nucleation occurs leading to aggregation, and polydispersed formation of nanoparticles which greatly affects the particle size, morphology and shape, and to avoid that a separation between the two stages is required i.e., nucleation and crystal growth do not occur concurrently. A uniform-sized distribution of the nuclei growth of nanoparticles is established when the formation of the nuclei occurs at the same time with the growth phase [57]. Co-precipitation is one of the simplest and commonly used chemical methods for acquiring nanosized Fe_3O_4. This is due to several advantages such as high yield, simple synthesis procedures, and requirements of non-toxic materials [58]. It is described as the occurrence of simultaneous ferric and ferrous iron salts precipitation in alkaline aqueous solution [47]. As shown in Fig. 1, a source of ferrous (Fe^{2+}) and a source of ferric (Fe^{3+}) is dissolved in water. Then, a weak base acting as a reducing agent such as sodium hydroxide or ammonia solution is added, resulting in the precipitation of iron oxide nanoparticles. The MNPs are washed with water and ethanol for several times to remove any impurities including excess ammonium or sodium salt. Later, the particles are dried forming iron oxide nanoparticles. The reaction takes place at room or elevated temperature

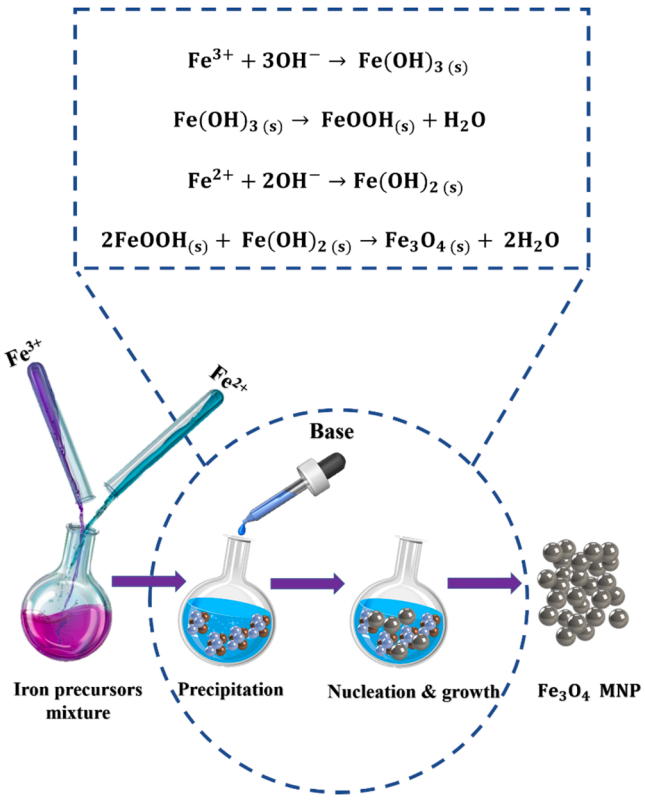

Fig. 1. A schematic sketch for the synthesis of iron oxide nanoparticles using chemical co-precipitation method. A source of ferrous (Fe^{2+}) and a source of ferric (Fe^{3+}) is dissolved in water. Then, a weak base acting as a reducing agent such as sodium hydroxide or ammonia solution is added, resulting in the precipitation of iron oxide nanoparticles.

(25–80 °C) under an inert atmosphere [59]. This reaction involves a complex mechanism of magnetite formation that takes place in different pathways however, the most dominant pathway is the topotactic akageneite transformation stage (crystal nucleus formation) to goethite stage (arrow-shaped nanoparticle formation) to magnetite [60]. Iron cations can easily oxidize in oxygen atmosphere which may lead to formation of an intermediate phase of iron oxide (i.e. goethite) around magnetite, forming a magnetite nucleus layered with goethite layer, and consequently forming a larger than expected nanoparticles [61] or it can undergo a critical oxidation forming maghemite. In order to protect the MNPs from oxidation, nitrogen gases bubbling through the solution is advisable. Moreover, applying nitrogen atmosphere while the process helps in reducing the particle size as compared to other methods in oxygen environment. Moreover, the dissolved oxygen reacts with hydrazine solution (oxidation-resistant reagent) to form $[NH_3OH]^+$ which in turns react with Fe^{2+} to form magnetite as follows [62]:

$$N_2H_4.2H_2O + 4H^+ + \frac{1}{2}O_2 \leftrightarrow 2[NH_3OH]^+ \quad (1)$$

$$3Fe^{2+} + [NH_3OH]^+ + 6OH^- \rightarrow Fe_3O_4 \quad + [NH_4]^+ + 3H_2O \quad (2)$$

The synthesized MNPs size, shape and quality are affected by many factors such as precursor type and precursor ratio, pH and ionic strength, alkaline solution addition rate, reaction temperature [60,63,64], and the use or absence of stabilizing agent [37]. These distinct reaction parameters might result in the formation of different forms of MNPs [65].

The variation of using different ratios of ferrous ions (Fe^{2+}) to ferric ions (Fe^{3+}) influences the size of iron oxide nanoparticles. It was observed that larger particle size of 37 nm has resulted when using ferrous salts only, compared to a size of 9 nm when using both ferrous

and ferric salts.[63]. Increasing the ratio of Fe^{2+} / Fe^{3+}, increased the hydroxide large particles formation as a precursor of Fe_3O_4 which resulted in an increment of the size of Fe_3O_4 (from 9 to 37) nm. The stoichiometric ratio 1:2 of Fe^{+2}: Fe^{+3} in absence of oxygen would yield a complete precipitation [62].

In chemical co-precipitation, controlling of the particle size and distribution becomes difficult at a fast precipitation rate. However, a controlled nanosized iron oxide nanoparticles were synthesized with using co-precipitation technique by maintaining a highly stable pH level throughout the reaction [66]. The mean size of the synthesized nanoparticle were controllable over one order of magnitude (2–15 nm) when adjusting the ionic strength and pH of the precipitation medium. In addition, pH and ionic strength affect the electrostatic surface charge of the particles by affecting the chemical structure and the surface of the particles and negatively impacting the uniformity and the monodispersed formation of nanoparticles [62]. Therefore, a smaller nanoparticles size is obtained under higher pH and ionic strength conditions [34] where a complete precipitation is expected to occur when the pH of the reaction is kept in the range of 8–14 [62].

The addition rate of the alkaline solution can significantly affect the formation process of the iron oxide nanoparticles. Generally, the magnetite nanoparticles produced by co-precipitation process at ambient temperature, are crystallized in a quasi-immediate process through a sophisticated mechanism resulting in various possible process routes. The reaction routes are dependent on the addition rate of the base solution to the iron salt mixture; a slow addition of the base to the iron chloride solution yields a nucleation of akageneite (β-FeOOH) followed by a transformation through goethite to magnetite. However, at higher rates of addition, different route competes with the previous one, where the ferrous hydroxide is nucleated then transformed to magnetite through lepidocrocite. This is due to the inhomogeneity of the reaction pH which existed before reaching a homogeneous mixing. In the vast majority of co-precipitation reactions, the various magnetite formation routes occur, however the topotactic transition of goethite to magnetite is the dominant process [60].

The reaction temperature affects the crystallinity of the synthesized magnetic iron oxide nanoparticle. Amorphous hydrated oxyhydroxide which simply converts to Fe_2O_3 is produced in the precipitation reaction at temperature less than 60 °C. However, Fe_3O_4 is formed at a temperature above 80 °C [62]. The saturation magnetization values of MNPs produced by chemical co-precipitation method is (30–50 emu/g) which is less than the bulk value (90 emu/g) [67]. This can be explained due to the poor crystallinity since the reaction temperature does not exceed the boiling point of water [68].

Stabilizing agents are usually used to enhance the size distribution of the prepared MNPs. This includes various surface ligands, such as surfactants, inorganic/organic molecules, and polymers. A lot of research has been conducted to employ stabilizing agent in the preparation of magnetic iron oxide nanoparticles for obtaining steady, uniform, fine, and crystalline particles using chemical co-precipitation method [69–71]. In addition, to overcome the instability of the Fe_3O_4 particles obtained by this method, a low molecular weight surfactants or functionalized polymers can be used. Precipitation homogeneity and monodispersity could be enhanced when the synthesis process involves a separation stage between the nucleation and growth steps. This occurs when a short eruption of nucleation occurs at the critical supersaturation concentration of the species, and by providing a slow growth of the nuclei by solutes diffusion on the crystal surface. This can be achieved by coating Fe_3O_4 nanoparticles with carboxylate surfactants, including, lauric acid, oleic acid (OA), or citric acid during co-precipitation reaction followed by dispersion in organic medium. Dodecyl benzene sulfonic acid sodium salt (NaDS) could be used as well to inhibit particles agglomeration [52].

2.2. Thermal decomposition

Thermal decomposition is a chemical reaction where heat is a reactant which is required to decompose the chemicals used in the reaction. This technique was introduced to deal with non-aqueous solvents and to address the shortcomings of co-precipitation synthesis method by producing highly monocrystalline and monodispersed magnetic nanoparticles. Generally, thermal methods are based on the utilization of high temperature processes to acquire iron oxide nanoparticles from metalloorganic compounds. The most common process is the thermal decomposition of salts containing Fe from a non-aqueous mixture in closed system and under inert atmosphere as shown in Fig. 2 [39]. In such process iron precursor (iron acetylacetonate, iron carbonyls, and iron cupferronates) is decomposed in a high temperature organic solvent in the presence of stabilizing surfactants (oleic acid, oleyl amine, and steric acid). This reaction is considered endothermic since it absorbs thermal energy to break chemical bonds between particles. This method produces high-quality MNPs characterized by their increased crystallinity, controllable properties, and small sized particles with an average size of 15 nm [72].

There are two pathways for the precursor's insertion process into the reaction. The first is done by simply mixing the precursors and surfactants at room temperature and then begin heating up according to a specified protocol [73]. Iron acetylacetonates and iron-oleate complex are commonly decomposed using this procedure. The second approach is hot injection, where the solution is heated in the existence of surfactants and the precursors are then injected, causing the instant nucleation and growth process of MNPs. This mechanism is usually applied for the decomposition of metal carbonyl precursors. Furthermore, MNPs generated from the thermal decomposition technique are generally coated with hydrophobic ligands, making them insoluble in water. Therefore, an additional step involving surface modification is necessary to provide MNPs with solubility in water to be suitable for implementation in water treatment applications.

Surface modification is performed either by ligand addition or ligand exchange [67,73]. In the ligand addition method, amphiphilic ligands are used, which facilitate organometallic reactions in water. This is possible by the attachment of the hydrophobic part of those amphiphilic ligands with the hydrocarbon chains of MNPs by hydrophobic interactions. This results in a two-layered structure with the hydrophilic segment directed towards the outer side of MNPs thereby turning it into water-soluble particles. However, the ligand exchange approach depends on the direct substitution of original hydrophobic molecules by a new hydrophilic ligand. Those ligands have two functional groups, the first is responsible for the attachment of molecules to the MNPs surface by strong chemical bonds, while the other functional group has a polar character, allowing the MNPs to be dispersed in water or be further functionalized. A successful synthesis of a monodispersed and highly crystalline MNPs can be acquired by thermally decomposing iron pentacarbonyl acting as organometallic precursors, and oleic acid surfactant at 100ºC without size-selection process [74]. This leads to the oxidation of the resulting iron-oleic acid metal complex to form maghemite (ɣ-Fe_2O_3) particles using a mild oxidant, trimethylamine oxide. Similarly, iron oxide nanocrystals were obtained by the decomposition of iron chloride in the presence of sodium oleate surfactant at 317 ºC [75]. Furthermore, thermally decomposing Fe^{+3} acetylacetonate in phenyl/-benzyl ether and 2-pyrrolidone have yielded a high-quality MNPs with a size range of 3–20 nm. It was found that reaction parameters impact the size and morphology of the synthesized MNPs such as precursors type and concentration, capping agents, solvent type, reaction time and temperature, heating rate, and reagent ratio [58]. Thus, by tunning the size, mono-dispersion, and morphology of the product, nano-magnetite different structures (tetrahedrons, octahedrons, concave, multi-branches, plates, and self-assembled structures) can be obtained [76].

The particles size of the MNPs produced by thermal decomposition

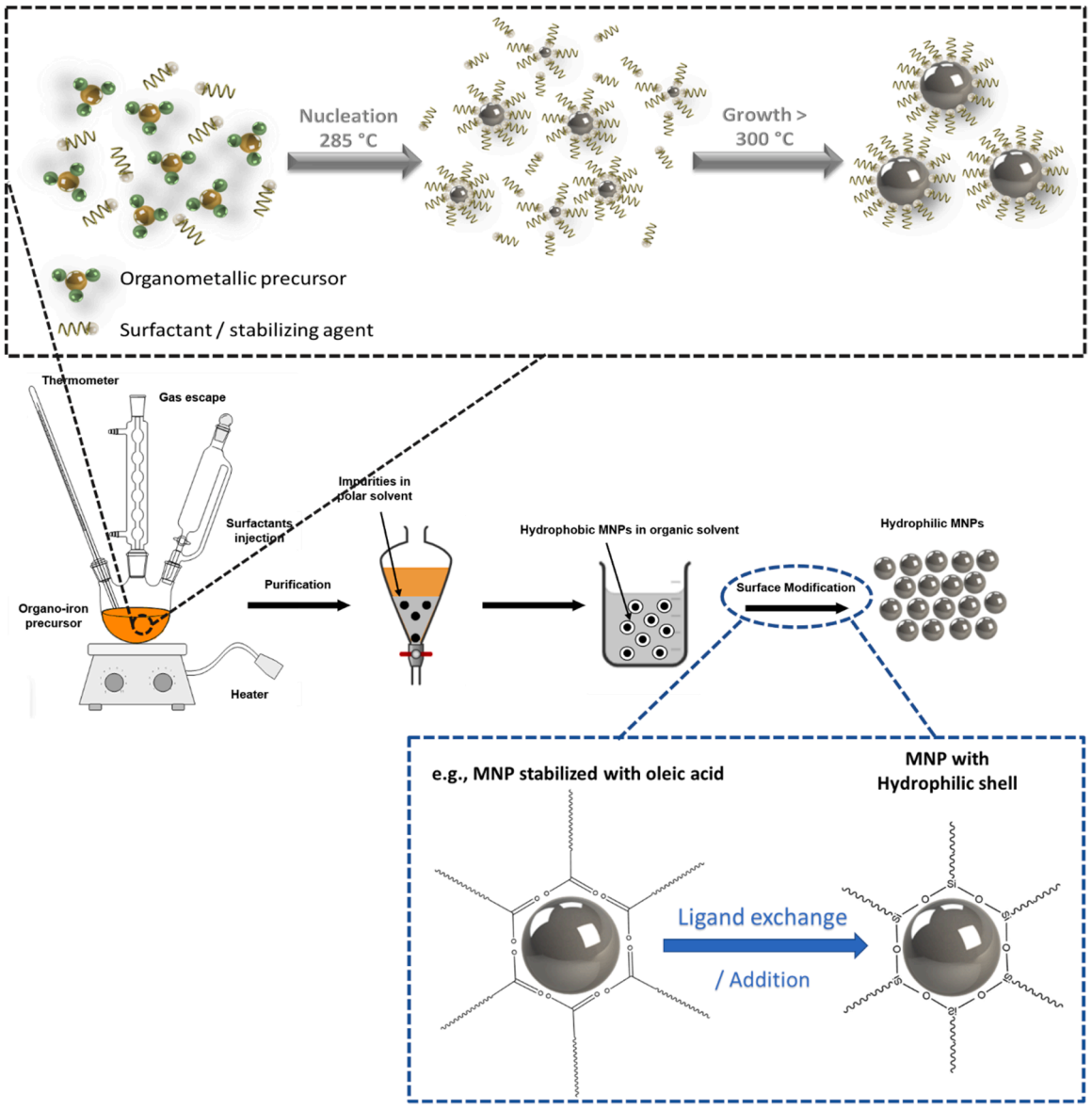

Fig. 2. A schematic sketch for the preparation of iron oxide nanoparticles using thermal decomposition method. Iron precursor is decomposed in a high temperature organic solvent in the presence of stabilizing surfactants. Surface modification is done to convert the MNPs from hydrophobic to hydrophilic, this is done by ligand addition or ligand exchange.

can be controlled by the precursor concentration and type, solvent type and concentration, and the use of stabilizing agent. Precursor concentration is an important parameter for tuning the MNPs size and shape. As the mean size of the nanoparticle increases with increasing the concentration of the precursor which is due to Ostwald ripening of smaller particles leading to larger particles formation. Moreover, the irregularity of the shape increases as well with increasing the precursor concentration. As the $Fe(acac)_3$ concentration increased from 0.1 mmol to 8 mmol, magnetite nanoparticles mean size increased from 2 nm to 7 nm [77]. In addition, the reaction time is directly proportional to the mean size of the nanoparticles yet, for a longer time durations (60–120 min) the size remains unchanged but broadens slightly which is possibly is a result of Ostwald ripening of the fine particles which in turn agglomerates and grow into larger particles [77]. Magnetite with diameters of 6.4, 7.7 and 9.0 nm for example, were obtained when the reaction lasted for 35, 45 and 60 min, respectively [78].

The type of solvent used in this process affects the shape and size of the MNPs by affecting the boiling point. Since the boiling point of this process depends on the solvent boiling point. Therefore, to obtain smaller size of magnetite nanoparticles a lower boiling point are favorable, because nucleation and growth steps are difficult to separate at higher temperatures [78]. For example, this can be achieved by replacing 1-octadecene with the boiling point of 320 ℃ by 1-tetradecene and 1-octadecene mixture to get boiling point of 290 ℃. Usually, a spherical shape is obtained from this method however it can be tuned to cubical shapes through the addition of sodium oleate in the decomposition step [79]. Polyethylene oxide is widely used as a surfactant for agglomeration inhibition by offering steric stabilization for the MNPs however, MNPs shape was less spherical which could be due to the lack of good covalent interaction between PEO polymer chains and the iron precursor such as $Fe(acac)_3$. Therefore, oleic acid can be introduced to the synthesis process resulting in more spherical MNPs shape since oleic acid has –COOH functional group that can make a covalent bond with iron atoms. However, oleic acid concentration does not affect the mean size of the formed magnetite MNPs [77]. The solvent amount is another contributing factor affecting the size of the MNPs. It was observed that the more the amount of the solvent the less the concentration of the precursor which results in less particle size. PEO serves as a solvent, and

when it was increased from 10 mL to 20 mL the particle size was decreased from 9 nm to 7 nm, respectively [77].

Although the main advantage of this process is the production of highly crystalline MNPs which is because of reaching higher temperatures, mono-dispersity, the ability to control the particles shape, depending on the stabilizer type which controls the reduction rate of nanoparticles formation [39], and the high saturation and initial magnetic susceptibility of the particles [76]. However, a major disadvantage is the incapability of nanoparticles to be dissolved in polar solvents [47]. Moreover, the sequential surface modification of the product may be less efficient and hampered due to the presence of residual surfactants. In addition, the MNPs biocompatibility is risked due to toxic solvents and surfactants employment [37]. It is also time, material and energy consuming with a limited production rate [47].

As shown in Fig. 3, thermal decomposition method produces less agglomerated MNPs [80]. However, the co-precipitation route remains to be more favorable rather than thermal decomposition owing to its high yield, ability to produce water-soluble and dispersible MNPs, time and cost efficiency, and limited use the use of toxic or hazardous solvents or reagents. Additionally, it is a safer method since it does not need high temperature or pressure unlike thermal decomposition route. However, it lacks the control over the particle size, crystallinity, and thus magnetic properties that can be offered by thermal decomposition routes [81].

3. Generation of osmotic pressure using MNPs and the mechanism in FO process

FO operates based on the osmotic pressure gradient between the feed and draw solution. The osmotic pressure of a solution is usually calculated using Van't Hoff equation (Eq. (3)).

$$\pi = iCRT \tag{3}$$

Where i is the dimensionless Van't Hoff index, C is the concentration of solute (mol/L), R is the ideal gas constant (L.atm/mol.K) and T is the solution temperature (K). The Van't Hoff index for magnetic nanoparticles is 1, because it does not dissociate in water. Van't Hoff equation turns out to be only a very rough approximation of the real osmotic pressure, especially for particles that do not dissociate in the solvent [82]. However, it is worth mentioning that the coating layer attached to MNPs surface are able to protonate/deprotonate which enhances the osmotic pressure. The osmotic pressure can be estimated with other models like Donnan equilibrium after conducting the suitable simulation and modeling the system's equation [83,84]. Future studies might consider measuring the osmotic pressure of magnetic nanoparticles draw solution using Donnan equilibrium of polyelectrolyte solution. Recent studies however, measure the osmotic pressure of magnetic nanoparticles draw solution by an analytical method such as freezing point depression, the boiling point elevation, and the vapor pressure depression [85]. As shown in Fig. 4, the magnetic nanoparticles can be used as draw solute in the FO process to generate osmotic pressure. The osmotic pressure generated by the magnetic nanoparticles mainly depends on particle's surface charge, size, and hydrophilicity [86]. The nanoparticles attract the water molecules through the membrane pores, because of the higher concentration of the draw solution and the charges which are distributed on the surface of the nanoparticle. MNPs particles size can be controlled in the synthesis process, however the colloidal stability property dominates the particles size after the dispersion of particles in water [87]. A stable colloidal dispersion has high ability for the conservation of the original local structure and radius of curvature at the nano and atomic scales of the MNPs. MNPs has poor colloidal dispersion due to the dipole-dipole interaction between the particles. The particles stability can be improved by increasing the electrostatic repulsion between the particles, this can be done by coating the nanoparticles with a thin layer of surfactant or a coating polymer [88]. In addition, the coating layer provides shielding for the dipole-dipole interaction between the particles. The colloidal stability can be also affected by the pH of the solution due to its effect on the surface charge of the particles [89]. It is worth mentioning that the coating agent must

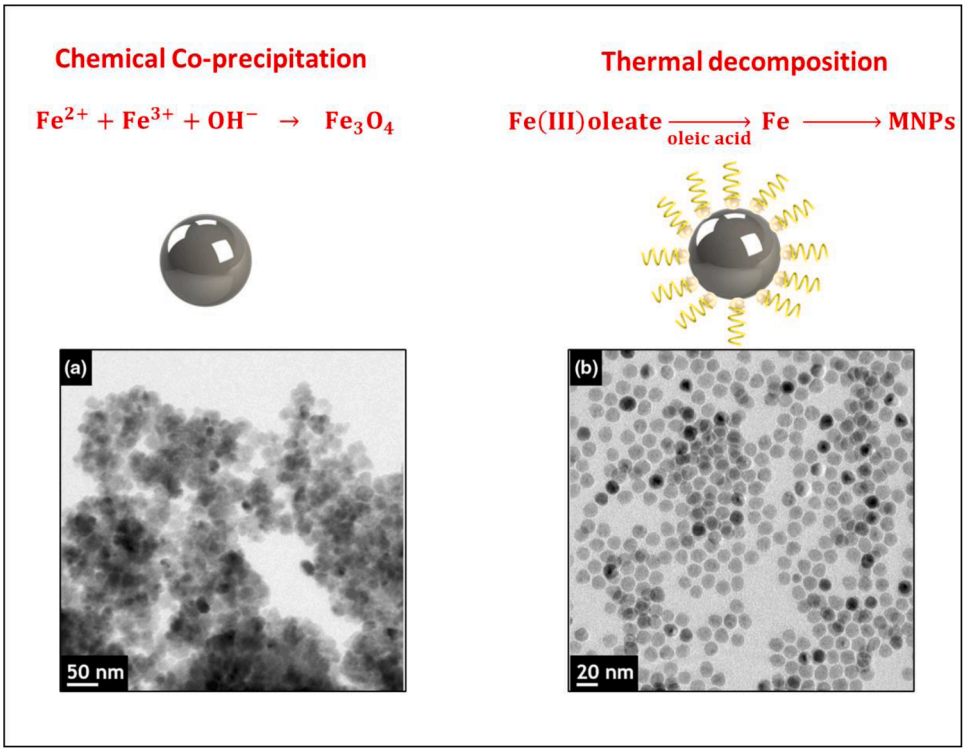

Fig. 3. A schematic sketch and TEM images showing the difference between the chemical co-precipitation and thermal decomposition processes [80]: (a) TEM of MNPs synthesized using chemical co-precipitation method (b) TEM of MNPs synthesized using thermal decomposition method. It can be inferred from the figure that the MNPs produced by the chemical co-precipitation are more agglomerated compared to the MNPs synthesized suing thermal decomposition method.

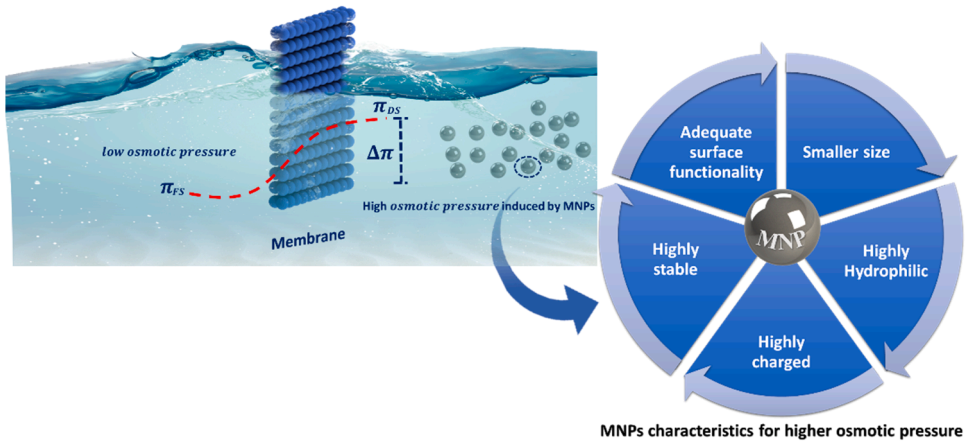

Fig. 4. A schematic sketch showing the pure water diffusion through the forward osmosis membrane pores due to the osmotic pressure gradient generated by the magnetic nanoparticles in the draw solution, and factors controlling the osmotic pressure generated by magnetic nanoparticles.

be hydrophilic to enhance the colloidal stability of the MNPs. A detailed discussion about the effect of using different coating on the MNPs will be provided in the next section of this study.

The water flux in the FO process is generated by the osmotic pressure gradient between the FS and DS. As shown in Fig. 5, the FO membrane is composed of two layers, the active layer with high rejection and selectivity abilities, and highly permeable support layer. The FO process can be operated in two modes of operation; (1) FO mode where the active layer is placed towards the FS and the support layer is placed toward the DS, (2) PRO mode where the active layer is placed towards the DS and the support layer is placed toward the FS. It was found that higher flux is usually obtained when operating the process in PRO mode compared to FO mode. This is attributed to the concentration polarization phenomena which is more severe in the FO mode compared to the PRO mode [90,91].

4. Modified MNPs used as FO draw solute

Bare MNPs have been rarely used as draw solution in the FO process due to low water flux and poor colloidal stability [92,93]. Therefore, the MNPs are coated using various types of material mainly including polymers (synthetic or natural) or other organic and non-organic coatings. This is done to reduce the agglomeration, enhance the stability, and modify the properties of the MNPs to meet the targeted DS characteristics. The choice of coating agent is critical since it hugely affects the water flux of the process as shown in Fig. 6. The performance of each coating agent was analyzed in this section to provide recommendations for designing efficient MNPs to be used as DS in the FO process.

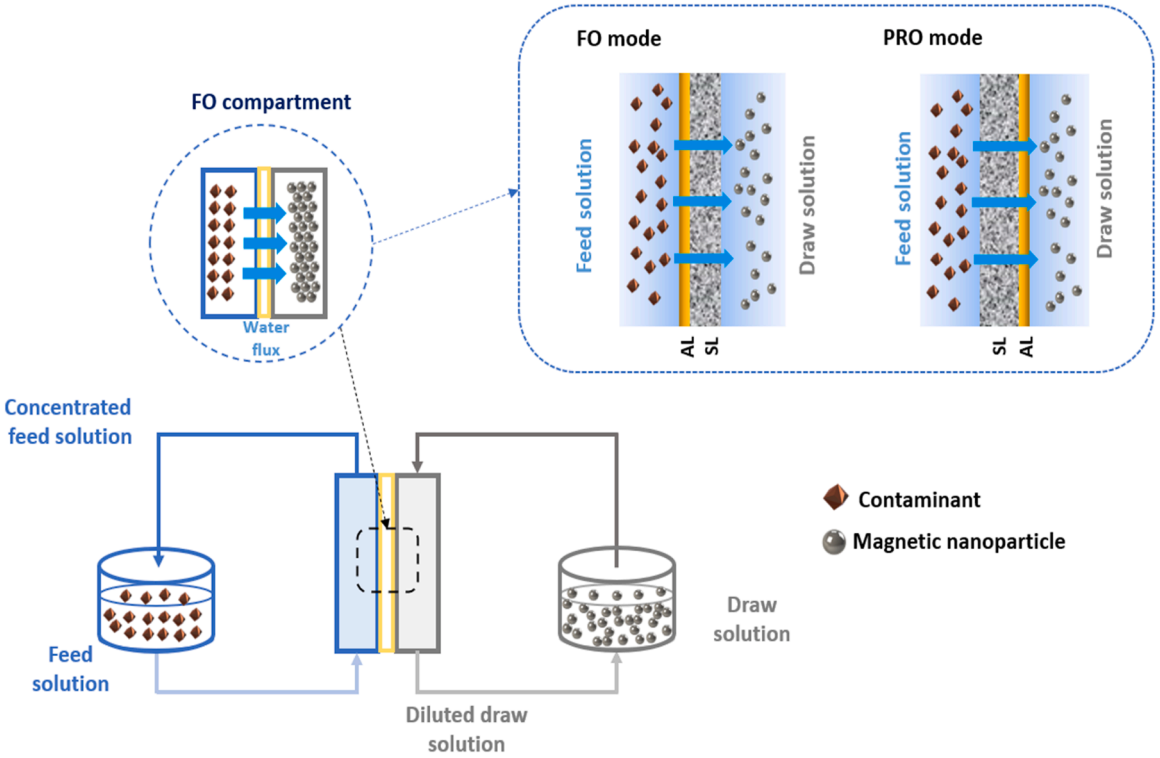

Fig. 5. Forward osmosis process and modes of operation. The pure water flux diffuses through semipermeable membrane from low osmotic pressure feed solution to a higher osmotic pressure draw solution. The FO process can be operated by two modes, FO mode where the active layer of the membrane is placed toward the feed solution, and PRO mode where the active layer of the membrane is placed toward the draw solution.

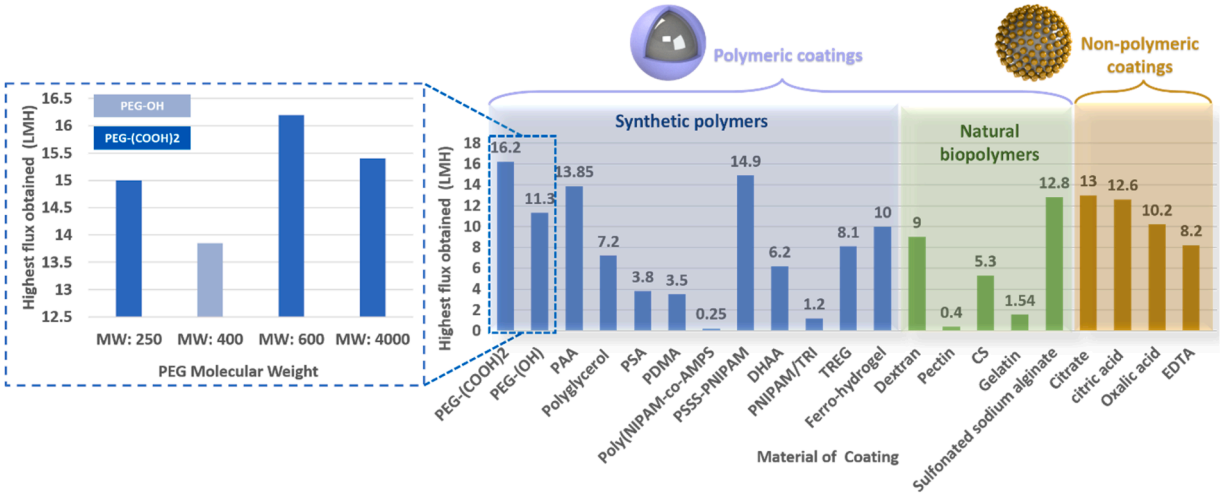

Fig. 6. A graphical illustration showing the maximum water flux generated by various polymers done in previous studies PEG-$(COOH)_2$ [94], PEG-(OH) [95–97], PAA [98], Polyglycerol, PSA [99,100], PDMA [101], Poly(NIPAM-co-AMPS) [102], PSSS-PNIPAM [103], DHAA[104], PNIPAM/TRI [105], TREG [106,107], Ferro-hydrogel [108], Dextran [109], Pectin[110], Chitosan [104], Gelatin [111], Sulfonated sodium alginate[112], Citrate[113], Citric acid [114], Oxalic acid [114],and EDTA [114].

4.1. Polymeric coated MNPs

In forward osmosis, the polymers are chosen on the basis to create high osmotic pressure, reduce the particles agglomeration, and minimize the membrane fouling. Therefore, the coating polymer must be very thin, stable, and should have high ionization capacity and similar charge to the membrane. To date, various polymers has been used as coating agents for magnetic nanoparticles draw solution including polyethylene glycol, polyacrylic acid, polyglycerol, poly sodium acrylate, Poly [2- (dimethyl amino) ethyl methacrylate] as synthetic polymers, and dextran, pectin, chitosan, gelatin, and sodium alginate as natural biopolymers.

4.1.1. Synthetic polymers coatings

4.1.1.1. Polyethylene glycol. Polyethylene glycol (PEG) is widely used in various biological and chemical applications due to its low toxicity and hydrophilic nature [55]. PEG with various functional terminal groups have been utilized as a coating polymer for MNPs draw solute in the FO process, this includes PEG terminated with dicarboxylic group [94], and hydroxyl group [95,97]. PEG-$(COOH)_2$ was used as a surface ligand to stabilize the iron oxide nanoparticles due to the chemically inert hydrophilic polyether chain and two reactive carboxylic acid moieties [94]. The carboxylic group has high reactivity towards the iron metal, which enhances the bonding process with the iron oxide nanoparticles. In addition, it is favored for the nontoxic nature, good water solubility, and high boiling point. The MNPs were synthesized using thermal decomposition method using Tris(acetylacetonate)iron (III) as source of iron and Triethylene glycol as a solvent, the PEG-$(COOH)_2$ was attached to the iron oxide core by physical adsorption. Higher water flux was obtained using smaller particles, where larger amount of grafting agent was attached to the surface of the MNPs when the particles became smaller. The particle size decreased as the ratio of PEG-$(COOH)_2$: Fe $(acac)_3$ increased. The mean diameter of the coated MNPs decreased from 13 nm to 4 nm as the ratio of PEG-$(COOH)_2$: Fe$(acac)_3$ increased from 1:2–4:1. In addition, the particle size was affected by the molecular weight of the coating polymer, where the particle size was 11, 14, and 18 nm when using [PEG-$(COOH)_2$ MW:250], [PEG-$(COOH)_2$ MW:600], and [PEG-$(COOH)_2$ MW:4000], respectively. As a result, the water flux was 13.5, 13.0, and 11.6 LMH when using [PEG-$(COOH)_2$ MW:250], [PEG-$(COOH)_2$ MW:600], and [PEG-$(COOH)_2$ MW:4000], respectively. This is due to the smaller size of the particle obtained at lower molecular weight, more specifically the osmotic pressure increased at smaller particle size due to the higher surface area: volume ratio. The water flux decreased after recovering the nanoparticles using a magnetic force, where the water flux decreased from 13 LMH to 10.5 LMH after 9 running cycles due to the agglomeration. There was no reverse diffusion of the particles through the membrane because the conductivity of the feed solution after the experiment was equal to the conductivity before the experiment. The magnetic saturation decreased from 68.1 emu/g for bare MNPs to 52.8, 35.5, and 22.0 emu/g for [PEG-$(COOH)_2$ MW:250] MNPs (1:2), [PEG-$(COOH)_2$ MW:600] MNPs (1:2), and [PEG-$(COOH)_2$ MW:4000], respectively. It was noticed that MNPs with particle size higher than 20 nm became ferromagnetic and remined magnetized. To further enhance the osmotic pressure generated by PEG coated MNPs, a hollowed MNPs was stabilized using PEG terminated with hydroxyl group [97]. The MNPs had an average particle size of 12 nm synthesized using thermal decomposition method using Iron oxy hydroxide as source of iron and 1-octadecene as a solvent. The synthesized MNPs were hollowed by acid etching method using trioctylphosphine oxide as agent and coated by PEG (MW 5000) terminated with hydroxyl group using ligand exchange method. The water flux was evaluated using U-tube apparatuses at an experimental time of 4 h. The maximum water flux was 1.16 LMH, obtained using PEG coated MNPs as draw solute at a concentration of 1.8 g/L. There was no reverse diffusion of the particles through the membrane which was confirmed by measuring the concentration of iron in the feed solution after the experiment. The magnetic saturation of the synthesized PEG coated MNPs was almost 40 emu/g. In another study, MNPs coated with PEG (MW 4000) was used as draw solution for the concentration of urine by forward osmosis [95]. The MNPs were synthesized using co-precipitation method at 80 °C using iron chloride (II) as source of Fe^{+2}, iron chloride (III) as a source of Fe^{+3}, and sodium hydroxide as base. PEG was added to the solution after the precipitation stage and stirred vigorously, then treated using ultrasonication to decrease the agglomeration of the MNPs and stirred again. Theoretically, 10 g of Fe_3O_4 was coated using 2.5 g, 5 g, and 40 g of PEG to obtain a coating ratio of 1:0.25, 1:0.5, and 1:4, respectively. The actual coating percentage was found to be 3%, 6%, and 31% when using 2.5 g, 5 g, and 40 g of PEG, respectively. The maximum coating ratio increased from 31% to 40% when placing the particles under sonication for 30 min and stirred again due to the reduction in particles agglomeration. The average water flux in the FO process was almost 1 LMH using a draw solution concentration of 9.6 g/L and urea as a feed solution, the water flux could be enhanced by increasing the

concentration of draw solution. However, it is worth mentioning that PEG coated MNPs produced higher water flux compared to the same amount of PEG. This could be attributed to the fact that contained electrolytes produce stronger osmotic pressure than free uncontained electrolytes. The PEG-coated MNPs was recovered and reused as DS, the water flux decreased by 7% after 3 cycles.

4.1.1.2. Polyacrylic acid. Polyacrylic acid (PAA) is a synthetic, non-toxic, high molecular weight polyanion, where each unit has carboxyl moiety, polymer. It is a weak polyelectrolyte which has a different degree of dissociation that are pH and ionic strength dependent. Its solubility in water and high reactive functional groups density makes it attractive in FO applications [115]. Since MNPs agglomeration is a real struggle, huge efforts were conducted to obtain the desired and necessary stability and dispersion of the MNPs, where carboxylate compounds are used as a possible stabilizing agent which makes PAA stabilize MNPs through electrostatic and steric repulsion against aggregation [116]. Hydrophilic PAA coated MNPs' (HMNPs) potential as a draw solute was investigated and compared with PEG coated MNPs. Various diameters of HMNPs were synthesized using PAA functional groups by employing different PAA: metal precursor ratios using thermal decomposition method where $Fe(acac)_3$ was used as a metal precursor. Different amounts of PAA were dissolved in 25 mL Triethylene glycol with nitrogen gas flow to obtain an oxygen-free reaction flask, then $Fe(acac)_3$ was added to the reaction flask and heated to 190 °C then to 275 °C [117]. The size of the MNPs decreased from 30 nm to 8 nm when PAA amount increased, and when the concentration of PAA MNPs as a draw solute used in DI water increased from 0.02 to 0.08 M, the water flux increased from 6.86 LMH for the MNPs synthesized with higher PAA concentration. At the same draw solute concentration, PAA coated MNPs had higher water flux than PEG coated MNPs since PAA coated MNPs are smaller in size. This is attributed to the larger surface area that is offered by the smaller size of the particles relative to the volume which results in higher osmotic pressure that can extract water from the same feed solution volume (DI). Additionally, the smaller the size of the MNPs, the more MNPs existing in unit volume thus, the higher the induced osmotic pressure. However, there is a drawback of using smaller sizes MNPs which is the weakness of its magnetization due to increasing the hydrophilic polymer wrapped around the magnetite cores. As a result, unsatisfactory results of MNPs recovery were obtained since the diameter of the particles was out of the range that the magnet can capture. Thus, a compromised size of MNPs should be used between the choices of high-water flux and ready recovery by the magnetic field. Even though there is an algorithmic relationship between the water fluxes and the pressure, the relation between the molar concentration and water fluxes was non-linear since the relation between them was not proportional. This could be attributed to ICP effect in FO asymmetric membrane. Another viable cause for the water flux non-linear increment, could be the strong hydrogen bond between the OH groups in the FO membrane and the carboxylate groups in PAA polymer chains. This would result in adhering the HMNPs to the surface of the membrane causing a partial blockage of the membrane pores resulting in diminution of the flux. In addition to the above-mentioned reasons, increasing the PAA concentration in DS would result in increasing the viscosity which also negatively affect the water flux and its logarithmic enhancement. Moreover, it was also found that increasing the salinity of feed solution decreased the flux in a non-linear relationship yet a logarithmic correlation considering increasing DS effect. The recovery of the HMNPs was readily done by applying electromagnet from the side of the DS making these MNPs recyclable to be reused again as a DS in FO system. However, the flux decreased after a consecutive number of cycles due to the aggregation occurred as a result of the high electromagnetic strength [117]. MNPs were synthesized and functionalized using various chemical groups with an average size of (20−30) nm to explore the effect of surface chemistry on the osmolality and water flux in FO and PRO modes [106]. It was found that polyacrylic acid coated MNPs were smaller in size with an average diameter of (4−30) nm achieving the highest osmolality and larger potential chemical gap, thus a higher water flux. The chemical potential energy for water is 1309.5 kcal/mol, 2-Pyrol is 1405.5 kcal/mol, TREG is 1430 kcal/mol, and PAA is 1881 kcal/mol. Therefore, the highest chemical potential gap was obtained when using PAA as coating agent for the MNPs. PAA coated MNPs were easily captured using high-gradient magnetic separator (HGMS), and these MNPs were employed again as DS after their recycling. A slight flux drop was observed which is due to aggregation caused by HGMS. Yet, they are still soluble in water which confirms the firmly anchored carboxylate groups on the magnetite's surface [106]. Another polyacrylic acid coated MNPs was used as draw solute for concentrating protein rich solution using FO process [107]. The water flux achieved in the process was low, therefore a second stage concentrating process was done using brine as DS.

4.1.1.3. Polyglycerol. Hyperbranched polymers are categorized with spherical branch-on-branch structure that is usually formed through AB2 structure monomers' polymerization, evading cross-linking reactions throughout the polymerization process. Through an oxy anionic ring-opening polymerization of latent AB2 monomer (glycidol), a structure of an aliphatic polyether is obtained with hydroxyl end groups known by Hyperbranched polyglycerol. It can be synthesized with a ranged molecular weight between 300 and 700,000 g/mol. In analogy with linear poly (ethylene glycol), Hyperbranched polyglycerol owns a dense molecular structure and is more biocompatible. Magnetite nanoparticles were coated with Hyperbranched polyglycerol to obtain a water soluble (HPG-MNPs) (5.9 nm) by thermally decomposing $Fe(acac)_3$ in triethylene glycol (TREG), then it was modified with 8 mL of triethylamine and 4 g of succinic anhydride (SA). However, following this procedure is a multistep and requires a separation step through ultracentrifugation thus, scaling up would be hard. As a result, a one pot reaction synthesis of HPG-MNPs is suggested which is simpler and easily scaled up. In that procedure no separation of MNPs required before HPG grafting where TREG-coated MNPs have OH groups on its surface that induces grafting of HPG via glycidol ring-opening polymerization. HPG-MNPs are water soluble due to the polyglycerol surface that contains huge number of OH groups with an average hydrodynamic diameter of 21.16 nm. Consequently, The Succinate Functionalization of HPG-MNPs surface which was achieved through the OH group's reaction with succinic anhydride to obtain conjugate carboxyl groups, increased average hydrodynamic diameter to 23.98 nm, and the draw solute ionization capacity which in turns improved the draw solution's osmotic pressure and electrical conductivity therefore, it improved the FO performance. The osmotic pressure of the draw solute increased with increasing SHPG-MNPs concentration, and thus the water flux increased. However, at higher solute concentration of 400 g/L, the draw solution became saturated with SHPG-MNPs and formed a precipitate. In contrary to HPG-MNPs, which lacks carboxyl groups, the SHPG-MNP solution's osmotic pressure was two times the HPG-MNPs solution's osmotic pressure. As a result of the internal concentration gradient of the draw solute, the increase in the concentration of draw solute is not directly proportional to the water flux increase. SHPG-MNP recycling was done using ultra filtration pressure-dependent process for regeneration and reconcentration of the draw solute from the diluted draw solution instead of the external magnetic field separation, since it was reported that it could lead to aggregations of nanoparticles consequently, decreasing the water flux. After two recycling steps, a slight decrease in the water flux was observed. However, in contrary of the previously reported reports indicating leakage of coated magnetite after recycling step through UF membranes there was no significant loss of the SHPG-MNPs. This is due to the anti-fouling characteristic of the SHPG-MNPs coming from the hyper branched globular structure of the SHPG, and larger SHPG-MNPs' diameter than the pore diameter of the

UF membrane [118]. Moreover, to increase the efficiency of the draw solute, a carboxylation reaction was carried on to the HPG-MNPs surface with sodium chloroacetate to obtain Hyperbranched Polyglycerol Carboxylate-Coated Magnetic Nanoparticles (HPGC-MNPs) via one pot synthesis as well. Such modification had no change in magnetic properties, as compared to TREG-MNPs, size and morphology of nanoparticles which had an average diameter of 5.9 nm, and a hydrodynamic diameter of 29.5 nm. Same results and relation were obtained, however, at the maximum draw solute concentration of both HPGC-MNPs and SHPG-MNPs, HPGC-MNPs had a higher osmotic pressure than that of SHPG-MNPs. This is attributed to the higher COO–Na dissociation on the surface of HPGC-MNPs than that of COOH on SHPG-MNPs surface which improves the surface carboxylate groups ionization, and hence, increases the osmotic pressure. According to afore mentioned results HPGC-MNPs are better compared to SHPG-MNPs in the FO process, as a draw solute [119].

4.1.1.4. Poly-sodium acrylate. Poly sodium acrylate (PSA) is a chemical polymer made up of chains of acrylate compounds and it is known as water-lock due to the high capability of adsorbing water up to 100 times its weight [120]. The particles were synthesized by chemical co-precipitation method at a temperature of 80 °C using iron sulfate (II) as source of Fe^{+2}, iron sulfate (III) as a source of Fe^{+3}, and ammonium hydroxide as base. The particles were coated using polysodium acrylate using physical adsorption by dissolving the polymer into the solution before the nucleation stage. The coating ratio measured using thermogravimetric analysis was almost 45% when using a ratio of 1:1 (MNPS: polysodium acrylate). The highest water flux was 3.8 LMH obtained using a feed solution of distilled water and 7 g/L of poly sodium acrylate coated MNPs as draw solution. The membrane was visually inspected, and it was clear that the membrane fouling has taken place. The magnetic saturation of the poly sodium alginate coated MNPs was almost 25 emu/g.

4.1.1.5. Poly[2-(dimethylamine)ethyl methacrylate]. Poly[2-(dimethylamine)ethyl methacrylate] (PDMA) is multi-responsive polymer with a pH, thermal, and CO_2 stimuli. It can reversibly be protonated (hydrophilic state) or deprotonated (hydrophobic state) by CO_2 and N_2 purging [101]. In this study MNPs where synthesized through solvothermal approach then it was modified to Fe_3O_4 @PDMA via a sectioned fabrication methods as follows: NH_2 groups functionalization through APTES, Bromo isobutyl bromide (BiBB) amidification reaction to attain Fe_3O_4-Br initiator, and then at the final stage PDMA polymer chains growth via surface-initiated atom transfer radical polymerization (SI-ATRP). The Fe_3O_4 @PDMA was spherical in shape with a diameter of 42 nm with a mono-size distribution, possibly due to PDMA polymers protonation. The magnetic saturation values of Fe_3O_4 @PDMA-8 sample was 40 emu/g which has decreased from 60 emu/g for bare Fe_3O_4. Which is attributed to the organic layer on the Fe_3O_4 surface from PDMA. PDMA is a cationic polyelectrolyte at acidic conditions and anionic polyelectrolyte at basic conditions. By varying the content of PDMA on the Fe_3O_4 @PDMA surface, the pH of the draw solute, the CO_2 purging time on the FO water flux, the FO flux performance was studied. It was found that increasing the increasing the net PDMA coverage resulted in providing more hydrophilic groups and thus increased the water flux. Moreover, a considerable water flux was observed in acidic conditions due to the protonation and ionization of the dimethylamine groups which is the ionic functional groups of Fe_3O_4 @PDMA creating higher osmotic pressure. In addition, CO_2 purging time had a positive effect on the flux where increasing the purging time increases the flux. While purging CO_2 on the pH 10 solution that was giving unstable flux results, the flux had increased as well. This is attributed to the reaction of the PDMA backbone with carbonic acid causing protonation and thus, converting hydrophobic PDMA to hydrophilic PDMA. The Fe_3O_4 @PDMA was recovered through 2 steps as follows: 1) the dispersed MNPs were purged with N_2 in order to detach CO_2 and invert the dispersion state to aggregation stage which makes it easier to apply 2) external magnetic separation for the NPs recovery.

4.1.1.6. Poly(N-isopropylacrylamide-co-sodium 2-acrylamido-2-methylpropane sulfonate). Magnetic poly(N-isopropylacrylamide-co-sodium 2-acrylamido-2-methylpropane sulfonate) (Fe_3O_4 @P(NIPAM-co-AMPS)) nanogels was used as a draw solution in the FO process [102]. The iron oxide nanoparticles were prepared using chemical co-precipitation method and coated by P(NIPAM-co-AMPS) using physical encapsulation and precipitation polymerization. The polymer shell hindered the aggregation of particles and generated osmotic pressure. It was observed that the nanoparticles became less hydrophilic when the temperature increased due to the thermosensitive nature of P(NIPAM-co-AMPS). This property results in an improved regeneration efficiency using the magnetic force after the FO process. The performance of the synthesized nanogel was compared with magnetic poly(N-isopropylacrylamide-co-acrylic acid) (Fe_3O_4 @P(NIPAM-co-AA)). It was found that the water flux obtained using (Fe_3O_4 @P(NIPAM-co-AMPS)) was higher than the water flux obtained using (Fe_3O_4 @P(NIPAM-co-AA)). This is due to the strongly ionic sulfonate groups in the (Fe_3O_4 @P(NIPAM--co-AMPS)) and wide dispersion of the particles which induced higher osmotic pressure. The water flux obtained in the FO process using 0.02 g/mL (Fe_3O_4 @P(NIPAM-co-AMPS)) draw solution was almost 0.3 LMH and increased to 0.5 LMH and 0.6 LMH when the draw solution concentration increased to 0.05 g/mL and 0.1 g/mL, respectively. The magnetic nanoparticles were recovered using a permanent magnet under various temperature. It was found that the particles recovery was faster when conducted at a temperature of 65 °C compared to room temperature. This can be attributed to the thermosensitive monomer NIPAM introduced into the nanoparticles.

4.1.1.7. Poly(sodium styrene-4-sulfonate)-co-poly(N-opropylacrylamide). Polystyrene sulfonates are group of polymers used to remove potassium and calcium from solution at an industrial scale. It is a low-cost polymer with high solubility in water at room temperature. MNPs grafted with copolymer poly(sodium styrene-4-sulfonate)-co-poly(N-opropylacrylamide) (PSSS-PNIPAM) was synthesized and used as draw solute in the FO process [103]. The MNPs were designed on the basis of three basic functions, provide magnetic property using the iron oxide core, provide high osmotic pressure by the poly(sodium styrene-4-sulfonate), and high clustering abilities provided by the thermo responsive property of the (N-opropylacrylamide). The water flux obtained by the FO process was tested using a DS concentration of 33 wt%, and three different feed solution including deionized water, brackish water, and seawater. The water flux obtained using deionized water as feed solution was almost 15 LMH and decreased to 13 LMH after 5 running cycles. When using brackish water as FS, the water flux was almost 4 LMH and decreased to 3 LMH after 5 running cycles.

4.1.1.8. Ferro-hydrogel. Hydrogels are hydrophilic polymers with a crosslinked and 3D network that is capable of absorbing water when brought into contact with it. They ae able to swell and retain huge amount of water withing their structures [121]. The ability of swelling is attributed to the hydrophilic functional groups existing in their structure that is able to drain water into their matrix. Their biocompatibility, high water absorption capacity, nontoxicity, and ease of synthesis make them a considerable excellent FO draw agent. They undergo an alterable change in volume or transition solution−gel phase with temperature-stimuli to release the water absorbed [122]. One of hydrogel modification in FO application was to involve MNPs into its matrix to overcome the cost of hydrogel recovery in FO processes which is referred to as ferro-hydrogel [123]. Such modification enables the recovering of hydrogel through external magnetic field. A sensitive to external magnetic stimulus ferro-hydrogel was prepared and used as a FO draw agent using modified MNPs as a crosslinker [108]. Where, as

schematized in Fig. 7, MNPs were synthesized by co-precipitation, then functionalized with silica (SiO_2) using thin layer through sol-gel method (TEOS) to obtain Fe_3O_4 @SiO_2. Later, to modify the surface of Fe_3O_4 @SiO_2 with the polymerizable vinyl groups, it was functionalized with silane coupling agent, 3-(trimethoxy silyl) propyl methacrylate (MPS) so that the modified Fe_3O_4 @SiO_2 @MPS MNPs can be implemented as a crosslinking agent for poly (-acrylic acid-co-acrylamide) chains through free radical polymerization. Such chains exist since the ferro-hydrogel is synthesized through the polymerization of acrylamide and acrylic acid monomers. The evaluated performance of this study comparing between the prepared ferro-hydrogel and the 2 conventional: ferro-hydrogel, and crosslinked pure polymer hydrogel, via methylene bisacrylamide crosslinker. It is worth noting that in the conventional ferro-hydrogel, MNPs are only physically submerged within the hydrogel matrix (non-covalently bonded) which makes MNPs vulnerable to leaching out from hydrogel matrix causing hydrogel deficiency and MNPs loss [124]. The modified MNPs were 80 nm in diameter with a spherical morphology. The prepared ferro hydrogel had the highest water flux (10.2 LMH) and swelling ratio as compared to the others. Moreover, increasing the degree of swelling for all the three types of hydrogels decreases their water fluxes during the FO process. Using the prepared ferro-hydrogel there was no observed decrement in the performance of FO even after running 5 cycles. On the contrary other conventional hydrogels had a continuous decrease after each regeneration. The crosslinking points are formed by the Fe_3O_4 @SiO_2 @MPS nanoparticles in the prepared ferro-hydrogel, and hence incapable of leaving the hydrogel. In addition, since the nanoparticles are stationary, they are not prone to agglomeration regardless of the various conditions of their environment. Nevertheless, in conventional ferro-hydrogel, within a strong magnetic field, not only the magnetic nanoparticles are susceptible to building up or leaching out from the hydro-gel matrix, but also instigates a great reduction in water flux [108].

4.1.2. *Natural biopolymers coatings*

4.1.2.1. Dextran. Dextran is neutral bacterial, and biodegradable exo-polysaccharide, containing repetitive subunits of glucose. It is water and organic solvents soluble. Dextran coated MNPs were synthesized by chemical co-precipitation and the dextran was covalently bonded to the MNPs surface hydroxyl groups, and then used as DS for brackish water desalination using FO process. Brackish water was synthesized containing 2 g/L of $MgSO_4$ and used as feed solution. The dextran coated MNPs containing 64.44 wt% of dextran appeared as a spherical nanoparticle with an average uniform diameter of 30 nm. It was observed that the content of dextran also affects the size of the dextran coated MNPs, in which increasing the dextran content decreases the diameter of the coated MNPs. The highest water flux was almost 9 LMH obtained using 2.0 M of MNPs as draw solution in PRO mode. The MNPs were easily recovered using an external magnet due to the high magnetic saturation of the particles. The coated MNPs were highly dispersive in water therefore, a higher osmotic pressure was generated. However, after drying the dextran coated MNPs, its specific area went higher with a high surface energy as well which makes them vulnerable to aggregation [109].

4.1.2.2. Pectin. Pectin is a fruit waste product composed mainly of galacturonic acid chain and carboxylate and hydroxyl as functional groups, which makes it suitable for many foods production and medical applications [125]. Pectin coated MNPs prepared using chemical co-precipitation method has been used as draw solute in the FO process [110]. The pectin coating was attached to the MNPs using physical adsorption by dissolving pectin from the rind of Citrus or Apple in the solution during the nucleation of the iron oxide nanoparticles. The coating ratio measured using thermogravimetric analysis was 40%, and the water flux obtained using distilled water as feed solution and 2 wt% pectin coated as draw solution was almost 0.9 LMH. The magnetic saturation of the synthesized MNPs was 23.13 emu/g. Pectin coated MNPs draw solution was used for desalination of synthetic saline water [126]. The water flux was almost 7 LMH when using 1% NaCl feed solution and 0.5 wt% MNPs draw solution. As the concentration of pectin coated MNPs increased to 1.0 wt%, the water flux decreased to almost 3.0 LMH.

4.1.2.3. Chitosan. Chitosan is a biopolymer which is yielded as a by-product from the waste of shellfish industry, comprising natural polysaccharides. The alkaline deacetylation of chitin forms chitosan biopolymer, and chitin is a polymer obtained from crustaceans' exoskeleton. Chitosan is a non-toxic, hydrophilic, biodegradable and

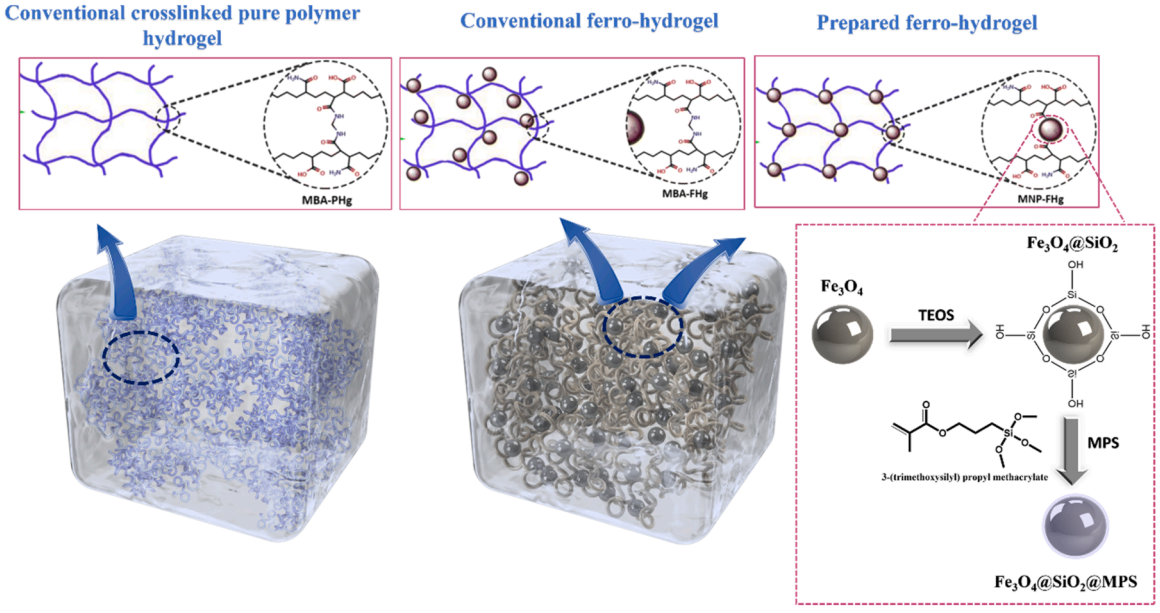

Fig. 7. A schematic illustration comparing between: conventional poly (acrylic acid and co-acrylamide) hydrogel and ferro-hydrogel where methylene bisacrylamide was used as crosslinker, (MNPs are attached physically on the polymer chains), and the prepared ferro-hydrogel (where MNPs were modified with TEOS and MPS to serve as a crosslinking agent for poly (acrylic acid and co-acrylamide) chains through free radical polymerization, (MNPs are chemically bonded within the hydrogel).

biocompatible, and inexpensive polymer with a molecular structure similar to cellulose, attracting a lot of attention due to such desirable characteristics [127,128]. Therefore, magnetic nanoparticles functionalized with chitosan has gained attention recently. Superparamagnetic chitosan coated MNPs were prepared by UV irradiation through partial reduction co-precipitation in an aquatic process approach. Their magnetic properties, agglomerations, size and chitosan content, and magnetic saturation depend mainly on the coating ratio (chitosan: Fe_3O_4) and the pH deployed. It was concluded that the size of the coated particle increases, and the magnetization decreases with increasing the (chitosan: Fe_3O_4) ratio however, magnetic stability was not affected. Moreover, increasing the pH, increases chitosan content, resulting in increment of the average chitosan coated MNPs diameter. Chitosan coated magnetite prepared by the classical co-precipitation approach also revealed same results adding to that, the XRD analysis showed that there was no change in iron oxide phase or the crystal structure after the coating which revealed the predominant phases, magnetite, same as the bare MNPs [128]. Crosslinking agents were used to form a stronger bond between chitosan and surface of MNPs. Chitosan coated magnetite were synthesized by ex-situ co-precipitation method where the Fe_3O_4 were synthesized prior to chitosan modification, and chitosan was crosslinked using various ratios of combined crosslinking agents; tripolyphosphate and sulphate. The ratio of (chitosan: Fe_3O_4), the crosslinking agents' ratio (TPP: Sulphate), and the time of crosslinking affected the physical properties of the coated MNPs. It was found that increasing the (TPP: sulphate) ratio results in smaller particle size with more spherical shape, and increased magnetite% over maghemite%. Moreover, crystallite size decreases and the particle size increase with increasing the duration of crosslinking process. Thus, their illustrated efficient ratios in terms of smaller size, dominance of magnetite phase, and particle morphology, where; (1:1), (5:1), and 3 h for (chitosan: Fe_3O_4), (TPP: Sulphate) ratios, and crosslinking time, respectively [129]. The performance of chitosan and dehydroascorbic acid-coated Fe_3O_4 nanoparticles to be used in the FO process as draw solutes, were evaluated by operating a lab-scale FO setup [130]. They were synthesized through co-precipitation approach then modified with ascorbic acid and chitosan to form dehydroascorbic acid and chitosan coated Fe_3O_4 nanoparticles, respectively. Particle's agglomeration was observed for Fe_3O_4 nanoparticles due to van der Waals forces existed among the particles. However, after surface modification, the particles were dispersed due to the decreased dipole-dipole interactions between the NPs. It was found that there was a slight decrease in the magnetic saturation of CS-Fe_3O_4 (70.3 emu/g) and DHAA-Fe_3O_4 (77.7 emu/g) nano particles as compared to bare magnetite nano particles (83.8 emu/g) additionally, a ferromagnetic behavior was observed for both coated magnetite nanoparticles. CS-Fe_3O_4 and DHAA-Fe_3O_4 draw solutions (~ 20 nm avg. size) were tested in FO mode illustrating that the draw solute concentration affects FO water flux proportionally which is due to the enhanced osmotic pressure caused by both coated MNPs. However, the water flux obtained using dehydroascorbic acid coated MNPs was higher than chitosan coated MNPs this is attributed to the higher hydrophilicity of the ascorbic acid than chitosan which results in a higher osmotic pressure. While using pure water as FS and a DS concentration of 0.06 g/L, the maximum water flux obtained using dehydroascorbic acid coated NPs was 6.2 LMH and the water flux obtained using chitosan was 5.3 LMH. The recovery system of this study was simple which was done by attaching a magnet to draw solution container and eventually the MNPs were attracted to that magnet and easily parted from the draw solution which is the main advantage of using MNPs as draw solute.

4.1.2.4. Gelatin. Gelatin is a natural non-toxic biopolymer with an outstanding biocompatibility and biodegradability, and high efficiency attributed to multifunctional groups presence (NH_2, COOH) in its chains. MNPs are coated with gelatin for different applications and depending on the application the effective coating diameter is varied from 70 to 900 nm through controlling the synthesis conditions [131]. Gelatin coated MNPs generally can be synthesized by chemical co-precipitation via two ways where gelatin is added in-situ or ex-situ, however, ex-situ addition is preferred since it was found that the final product had more gelatin preserved following this way and produced stabilized MNPs. This is due to losing the larger and uncertain gelatin parts while separation and washing steps once added via in-situ method [132]. It was observed that increasing the gelatin content results in size reduction of crystallite, and the reason behind that is the formation of the gel-like network when dissolving gelatin in a medium where the particles nucleation and growth takes place in voids or nano-cavities at the gelatin network. When decreasing gelatin concentration, the crystallite size increases due to the expansion of the network creating larger voids [131]. A gelatin coated MNPs were developed for the desalination of brackish water using FO process using a new gelatin crosslinker; Persicaria bistorta root extract instead of the common crosslinker; glutaraldehyde since it is expensive and toxic. It was found that magnetic saturation of the coated species was less than the bare ones which is due to the gelatin layer shielding effect. Response surface methodology was used to study the impact of the gelatin concentration on the osmotic pressure of DS. The osmotic pressure was at its highest (1.01 bar) for Persicaria bistorta root extract at concentrations of 7.90% w/v, and 15,000 mg/ of gelatin and draw solution, respectively. The highest water flux was 1.54 LMH using a gelatin coated MNPs as the draw solution, deionized water as the feed solution. By repeating the process for nine cycles, the initial water flux was decreased to 0.365 LMH. This is due to the super magnetic property of the MNPs which caused particles agglomeration [111].

4.1.2.5. Sulfonated sodium alginate. Sodium alginate is a low cost, low toxicity, and water-soluble biopolymer produced from brown algae. This characteristic makes it applicable in various applications including pharmaceutical, food manufacturing, and cosmetics. Sulfonated sodium alginate coated MNPs has been used as draw solute in the forward osmosis process for reclamation of treated wastewater [112]. The magnetite nanoparticles were synthesized using chemical co-precipitation method at a temperature of 80 °C using iron chloride (II) as source of Fe^{+2}, iron chloride (III) as a source of Fe^{+3}, and sodium hydroxide as base. The synthesized MNPs were coated with sulfonated sodium alginate by modifying the particle surface using silicon dioxide and later with 3(Chloropropyl) trimethoxy silane for an enhanced bonding with the sodium alginate. The coating ratio measured using thermogravimetric analysis was found to be almost 10%, this was obtained when using 1:1 ratio between the silica coated MNPs and sodium alginate sulfate. The highest water flux and reverse solute flux were 12.8 LMH and 1.5 g/m^2.h, respectively obtained using draw solution concentration of 60 g/L. The water flux was 10.7 and 7.1 LMH for concentrations of 40 and 20 g/L, respectively. The water flux decreased by 6% after the third recovery cycle using a permanent neodymium magnet. The MNPs were fully recovered by the permanent magnet which was confirmed by measuring the conductivity of the water. It was claimed that the SEM images of the used membrane show that there is no fouling on the membrane surface after conducting the recovery process for three times, however this is not enough to evaluate the effect of using sodium alginate coated MNPs as DS on membrane fouling. The magnetic saturation of the sodium alginate coated MNPs was 50.6 emu/g.

4.2. Other non-polymeric coatings

4.2.1. Citrates

Citrates are used in various pharmaceutical and beverage industries applications due to super hydrophilic nature and low toxicity [133]. Citrate has three carboxylic group and one hydroxy group; this makes it super hydrophilic due to the nature of the functional groups. Citrate coated MNPs has been used as draw solution in the FO process due to the

high hydrophilic nature [113]. The particles were synthesized by chemical co-precipitation method at a temperature of 80 °C using iron chloride (II) as source of Fe^{+2}, iron chloride (III) as a source of Fe^{+3}, and sodium hydroxide as base. The MNPs were stabilized using citrate by adding trisodium citrate to the solution of MNPs and mixed vigorously under a temperature of 95 °C. The citrate was attached to the magnetite nanoparticles due to the strong bonds between the surface of the particles and portion of the carboxylate groups which have strong coordination affinity for Fe ions, while the uncoordinated carboxylate groups extend into the aqueous solution, making the particles strongly hydrophilic. The increase of temperature resulted in an improved surface coating due to the formation of chelating bidentate interaction between the iron ions on the magnetite surface and the citrate carboxylic groups. The coating ratio measured using thermogravimetric analysis was 9.1%, this shows the mass percentage of surface coating to the bare iron oxide nanoparticles by comparing weight percentages before and after burning the MNPs at high temperatures. However, the osmotic pressure is created by the uncoordinated carboxylate groups on the surface of the coated MNPs. Therefore, conductometric titration was used to measure the effective carboxylate groups which contributes to the generation of the osmotic pressure. The density of the carboxylate groups on the surface of the MNPs was calculated to be 1.2 mmol/g. It can be inferred from the study that calculating the osmotic pressure created by the MNPs must be based on the density of the functional groups available on the surface of MNPs instead of estimating the osmotic pressure based on the content of the coating polymer. The initial water flux obtained using 20 g/L of citrate coated MNPs as draw solution was almost 17 LMH and decreased rapidly to 4 LMH approximately after 30 min. The rapid flux decline can be attributed due to the accumulation of MNPs on the support layer of the membrane, and the hydrogen bonding between the CTA membrane and the MNPs.

4.2.2. Hydro-acids

The Hydroxy acids, which also are known as poly-carboxylic acids, have more than two carboxylic groups. Moreover, they are able to present a single carboxylic group or hydroxyl group with a ketone. Hydro-acid complexes are composed of hydro-acid ligand(s) and transition metal(s), where it has a tetrahedral or octahedral structure in the transition metal center. The minimal reverse solute flux and smooth solute regeneration can be achieved by this extended structure via either nanofiltration or membrane dialysis processes. Furthermore, also illustrated that the osmotic pressure can be greatly increased by the existence of high numbers of hydrophilic carboxylic groups in hydro-acids structure. In addition, such features make hydro-acid complexes suitable to be draw solutes in FO process applications [134]. The synthetization of Hydro-acid-MNPs were done by a modified approach of co-precipitation under mild conditions in a one-pot reaction [114]. Using the same ratio of Fe^{+3}: Fe^{+2}: Hydro-acid of 2:1:2, and according to the following order OA-MNPs< CA-MNPs < EDTA-MNPs, the particle sizes increase. The size of the particle is heavily dependent on the ratio of the iron starting materials to hydro-acids. This study also showed that with the increase of ratio of CA, the size of the CA-MNPs becomes smaller. In addition, when increasing the ratio of Fe^{+3}: Fe^{+2}:CA from 2:1:2–2:1:8, the mean diameter of the resultant CA-MPNs decreases from around 40–21 nm. This shows that how the particle size can be controlled by varying the ratio of iron to hydro-acids during the synthesis process. At the room temperature all hydro-acid coated MNPs are superparamagnetic. the magnetization can be reduced by the hydro-acid coatings following the order of OA<CA<EDTA when the same ratio of iron starting materials is used. The hydro-acid-MNPs concentration for all hydro-acid-MNPs increases the osmotic pressure. Among them, the osmotic pressure follows the order of CA-MNPs4OA-MNPs4EDTA-MNPs at the same hydro-acid-MNPs concentration. This even is correlated with the number of the free carboxyl groups and the fraction of hydro-acids in hydro-acid MNPs. Table 2.

As mentioned earlier MNPs can be regenerated using an external magnetic force. However, it was observed that all the previous studies claim full recovery of the MNPs from the diluted draw solution based on visual observations only [86,94,109]. As observed in Fig. 8, it can be noticed that there are traces of MNPs remaining in the water. Slight number of papers reported weight loss occurrences of MNPs after few cycles of operation [135]. This can be referred to the poor performance of the regeneration process [135]. From the authors point of view, it is compulsory to measure the concentration of the MNPs by an analytical method to ensure that it is safe for the end application. The magnetic regeneration process can be enhanced by using electromagnets instead of permanent magnets as shown in Fig. 8b. Electromagnets have higher recovery efficiency due to the stronger magnetic field compared to the permanent magnet, also it is more applicable when applying the technology at an industrial scale. However, the electromagnets need electricity for operation which adds up to the operating cost of the process. Another way of enhancing the recovery of MNPs is synthesizing a thermo-sensitive magnetic nanoparticle (Fig. 8c). Thermo-sensitive MNPs tends to agglomerate when heated due to the properties of the coating polymer. The recovery efficiency of the agglomerated particles is higher than the recovery efficiency of the MNPs obtained when being dispersed in water. The recovery of MNPs can be also enhanced by using ultrafiltration after the magnetic recovery of the particles. It can be determined that MNPs draw solution are reusable to some extent depending on the particle's properties and the regeneration method. However, there is a huge research need for evaluating the life cycle assessment of MNPs synthesized by the most used synthesis methods.

5. Toxicity of MNPs and regulation for the water treatment applications

The application of MNPs has recently expanded in many sectors, which has arisen concerns regarding the risks of increased exposure to such materials, especially that not much investigation has been done in the toxicity assessment of the MNPs [136]. MNPs can reach humans bodily components through inhalation, skin penetration, digestion, or direct injection [137]. When used in water treatment applications, there might be a chance that the MNPs could reach to the human body by digestion. Therefore, it is crucially important to evaluate the negative impacts created by the MNPs on the human body if digested. MNPs could have a potential risk when interacting with organs in the human body [138,139]. These new challenges and complications led to the development of a modern branch of science called nanotoxicology [140]. Generally, nano-sized particles of any material are increasingly toxic compared to particles of larger sizes of the same matter [141]. Nano-sized particles can penetrate into body parts such as the nucleus where larger particles cannot reach, this results in the accumulation of these matters in human cells which could become toxic [142]. Standard categorization of MNPs based on risk assessment and ecotoxicology is still hampered by the absence of enough information [143]. However, several studies have concluded that toxicity of MNPs is influenced by many parameters such as particle size, structure, concentration, surface chemistry, biodegradability, and solubility [144,145]. The effects of the MNPs properties on the toxicity level is summarized in Fig. 9. In this section, we will assess the toxicity level of MNPs depending on the properties of the particles. Also, several mitigations are discussed to overcome such risks when employed in the FO process for water treatment applications.

MNPs were originally considered to be non-toxic as they biodegrade in the body by releasing ferric ion (Fe^{3+}), which can get into the iron metabolism process. However, numerous studies have disclosed the possible toxicity of MNPs when accumulating inside the cells [146]. Polymer coatings are usually applied on MNPs to prevent the agglomeration and enhance particles hydrophilic properties [147]. In addition, coatings are applied to MNPs to act as a shield to hinder the direct interaction with the body cells, leading to a decreased toxicity of these particles. Many studies have agreed that uncoated MNPs nanoparticles

Table 2
Previous studies done on the synthesis of MNPs for the application of draw solution in forward osmosis process.

Coating / Functional group	Synthesis Method	Particle size	Osmotic pressure	Membrane	Highest Flux	RSF	Recovery Method	Remarks	Ref
Synthetic polymer coatings									
PEG-$(COOH)_2$ (MW: 250, 600 and 4000)	Thermal decomposition method	4.2–21.5 nm (TEM)	55 – 73 atm	CTA (HTI)	16.2 LMH (FS: DI water and DS: 0.065 M of [PEG-$(COOH)_2$ MW:600] MNPs (1:2).	0	Magnetic	The water flux decreased by almost 21% after 9 cycles due to slight particles aggregation.	[94]
PEG (MW: 4000)	Chemical coprecipitation	–	4.9 – 14.9 atm	CTA (FTS)	> 1 LMH (FS: urine and DS: 9.6 g/L of MNPs)	0	Magnetic	The generated osmotic pressure was not enough to concentrate the urine.	[95]
PEG (MW: 5000)	Thermal decomposition method	12 nm (DLS)	14.6 Pa	Porifera	1.16 LMH (FS: DI water and DS: 1800 ppm of MNPs)	0	Magnetic	The water flux was improved using an oscillating magnetic field.	[97]
PEG (MW:400)	Thermal decomposition method	9–32.5 nm (TEM)	–	CTA (HTI)	11.30 LMH (FS: DI water and DS: 0.08 M of PEG coated MNPs. 5.56 LMH (FS: synthetic saline water and DS: 0.08 M of PEG coated MNPs and 35,000 mg/l as feed solution.	–	Electromagnet	The high strength of the electromagnets possibly caused a slight aggregation of magnetic nanoparticles after each cycle which dropped the flux after consecutive number of cycles.	[96]
PAA		8–30 nm (TEM)			13.85 LMH (FS: DI water and DS: 0.08 M of PAA coated MNPs. 6.33 LMH (FS: synthetic saline water and DS: 0.08 M of PAA coated MNPs and 35,000 mg/l as feed solution.				
PAA	Thermal decomposition method	–	6.0 atm	CTA (HTI)	–	0	–	The MNPs was used for the concentration of protein solution. The concentration of the diluted DS was retrieved using a second stage FO process.	[98]
PAA TREG 2-Pyrol	Thermal decomposition method	20 – 30 nm (TEM)	–	CTA (HTI)	10.4 LMH (FS: DI water and PAA-MNPs draw solution) 8.1 LMH (FS: DI water and TREG-MNPs draw solution) 6.3 LMH (FS: DI water and 2-Pyrol-MNPs draw solution)	0	High-gradient magnetic separator (HGMS)	Higher content of PAA covering each particle induces weaker magnetic property. Thus, smaller PAA-MNPs recovery result was insufficient since their diameters are out of the range that the HGSM can capture. A compromised MNPs size should be attained.	[106]
TREG	Thermal decomposition method	1–10 nm (TEM)	65–70 atm	CTA (HTI)	7 LMH (FS: DI water and DS: 0.23 mol/L of TREG coated NPs)	–	Magnetic / Ultrafiltration	PAA-NPs draw solutions are recyclable in FO–UF for five times for synthetic seawater desalination avoiding the increase in their sizes or decreasing their osmotic functionality.	[107]
PNIPAM/ TRI	Thermal decomposition method	9 nm (TEM)	–	CTA (HTI)	1.2 LMH in FO mode (FS: DI water and MNPs draw solution) 1.5 LMH in PRO mode	0	low-strength magnetic separation	The water flux was low and constant after regeneration for 5 cycles.	[105]

(*continued on next page*)

Table 2 (*continued*)

Coating / Functional group	Synthesis Method	Particle size	Osmotic pressure	Membrane	Highest Flux	RSF	Recovery Method	Remarks	Ref
					(FS: DI water and MNPs draw solution)				
HPGC	Thermal decomposition method	22 nm (TEM)	16 atm	CTA (HTI)	7.2 LMH (FS: DI water and DS: 500 g/L of HPGC-coated MNPs)	0	Ultrafiltration	Ultrafiltration was used for the regeneration of MNPs, because magnetic separation caused aggregation of NPs and reduction in water flux.	[119]
SHPG	Thermal decomposition method	23.98 nm (TEM)	10 atm	CTA (HTI)	3.0 LMH (FS: DI water and DS: 400 g/L of SHPG-MNPs)	0	Ultrafiltration	The MNPs was stable for 3 repetitive cycles.	[118]
PSA	Chemical coprecipitation, Oxidative Precipitation	4–34 nm (TEM)	10.8 atm	–	–	–	Magnetic	–	[99]
PSA	Chemical coprecipitation	4 nm (TEM)	8.8 atm	AIM (Aquaporin)	3.8 LMH (FS: DI water and DS: 7 wt% PSA-MNPs)	0.05 g/ m^2 h	Ultrafiltration	–	[100]
PDMA	Chemical coprecipitation	31–42 nm (DLS)	–	Thin-film composite (TFC) membrane	3.5 LMH (FS: DI water and DS: 0.04 wt% PDMA coated MNPs) at pH 3.	–	Magnetic	Fe_3O_4 @PDMA NPs showed considerable results for water flux in acidic environment. Increasing CO_2 purging time on the water increased the flux.	[101]
P (NIPAM-co-AMPS)	Chemical coprecipitation	10 – 20 nm (DLS)	3.3 atm	CTA (HTI)	0.25 LMH (FS: DI water and DS: 20 g/L of Poly (NIPAM-co-AMPS) coated MNPs)	–	Thermal – Magnetic	The MNPs were completely recovered using magnetic separation at 65 C.	[102]
PSSS-PNIPAM	Thermal decomposition method	5.2 – 10.5 nm (TEM)	55 atm	CTA (HTI)	14.9 LMH (FS: DI water and DS: 33 wt% MNPs). 3.7 LMH (FS: saline water and DS: 33 wt% MNPs) 2.7 LMH (FS: sea water and DS: 33 wt% MNPs)	–	Magnetic / Ultrafiltration	The water flux decreased by almost 10% after each cycle within 5 cycles. A water flux was still attained above 2 LMH after 5 cycles while using seawater as FS.	[103]
Ferro-hydrogel	Chemical co-precipitation / sol-gel method	80 nm (TEM)		TFC-FO	5.72 LMH FS: DI water and DS hydrogel with MBA crosslinker). 10 LMH (FS: DI water and DS: hydrogel with Fe3O4 @SiO2 @MPS crosslinker).	–	Magnetic	In high-strength magnetic field, MBA-FHg, magnetic nanoparticles are susceptible to aggregate or leach out from the hydrogel matrix	[108]
Natural biopolymer coatings									
Dextran	Thermal decomposition method	< 30 nm (TEM)	–	CTA (HTI)	9.0 LMH (FS: Synthetic brackish water and DS: 2.0 M of MNPs)	0	Magnetic	–	[109]
Pectin	Chemical coprecipitation	200 nm (DLS)	–	PES (Aquaporin)	0.4 LMH (FS: well water and DS: 2 wt% of MNPs)	–	Magnetic	The water flux obtained in the study was lower than other studies because the osmotic pressure of the used FS was high.	[110]
Pectin	Chemical coprecipitation	520 nm (DLS)		Porifera	7 LMH (FS: 1% NaCl synthetic solution and 0.5 wt% of MNPs) 3 LMH (FS: 1% NaCl synthetic solution and 1 wt% of MNPs)		Magnetic	–	[126]

(*continued on next page*)

Table 2 (*continued*)

Coating / Functional group	Synthesis Method	Particle size	Osmotic pressure	Membrane	Highest Flux	RSF	Recovery Method	Remarks	Ref
Chitosan DHAA	Chemical coprecipitation	> 20 nm (TEM)	–	CA/CTA	5.3 LMH (FS: DI water and DS: 0.06 g/L of CS coated NPs) 6.2 LMH (FS: DI water and DS: 0.06 g/L of DHAA coated NPs)	–	Magnetic	The water flux of DHAA coated NPs was higher than CS coated NPs due to higher hydrophilicity of the particle.	[104]
Gelatin	Chemical coprecipitation	40–70 nm (TEM)	–	CTA (HTI)	1.54 LMH (FS: DI water and DS: 14.3 g/L of gelatin coated NPs)	–	Magnetic	The water flux decreased to 0.365 LMH after 9 running cycles.	[111]
Sulfonated sodium alginate	Chemical coprecipitation	–	117.2 atm	CTA	12.8 LMH (FS: DI water and DS: 60 g/L of MNPs)	1.5	Magnetic	The water flux decreased by 6% after three regeneration cycles.	[112]
Non-polymeric coatings									
Citrate	Chemical coprecipitation	3–8 nm (TEM)	–	CTA (HTI)	13 LMH (FS: DI water and DS: 20 mg/L of NPs)	–	Magnetic	Magnetic field assisted FO module reduced the membrane fouling and improved the overall efficiency of the process.	[113]
Hydro-acids	One pot chemical co-precipitation reaction	CA: 21–40 nm OA: 33 nm EDTA: 50 nm (TEM)	CA ~ 68 atm OA~ 56 atm EDTA~ 40 atm	TFC-PES	12.6 LMH (FS: DI water and DS: 0.8 g/mL of CA coated MNPs). 10.2 LMH (FS: DI water and DS: 0.8 g/mL of OA coated MNPs). 8.2 LMH (FS: DI water and DS: 0.8 g/mL of EDTA coated MNPs). 8.5 LMH (FS: 3.5 wt% of NaCl and DS: 0.6 g/mL of CA coated MNPs).	(0.08–0.09) g/ m^2 h	Magnetic followed by membrane separation process (thin-film polyamide NF membrane).	In membrane separation process, a gas pressure of 4 bar was sufficient.	[114]

showed high toxicity at a concentration exceeding 10 mg/L. Surface coating attains declined toxicity of MNPs when compared to uncoated ones, because it results in an increased hydrodynamic diameter [148]. In addition, surface charged nanoparticles exhibit increased toxicity levels in comparison to the neutrally charged ones [149,150]. Highly charged MNPs were reported to have an increased cellular uptake causing more interaction within the human body and therefore classified as more toxic [151]. This finding must be considered carefully since the higher surface charge is a desirable trait for an enhanced draw solution performance in the FO process.

It can be inferred from the literature that most of MNPs toxicity assessment aimed to explore the potential application of those particles as safe MRI contrast agents in clinical diagnosis [152,153]. These assays were accomplished using animals that possess similar genetics and immunological responses to humans such as zebrafish and mice [154, 155]. Even though these studies are not directly linking the associated toxicity of those particles with the FO process, we will review some of that work to gain an insight about the toxicity level and possible negative effects of MNPs on humans. Table 3 compiles number of previous studies indicating the toxicological concerns of coated MNPs with an intended stress on the functional groups used in the available FO papers. It was noticed by various studies that an intake of an uncoated MNPs with a concentration exceeding 10 mg/L could result in behavioral change [156], and damage to the red blood cells when using a concentration of 25 mg/L [156,157]. Chitosan coated MNPs was found to be less toxic than bare MNPs [158], however an alarming concern was pinpointed due to the enhanced surface charge which increased their intercellular uptake [159]. PEG coated MNPs showed low toxicity even when used at high concentration of 100 mg/L [160], this is due to the low toxicity and biocompatibility of the PEG polymer. Polyglycerol coated MNPs showed no toxicity when used at a high concentration of 200 mg/L [161].

In general, the employment of the coated MNPs as draw solution in FO process encloses a regeneration step using a strong magnetic field to assure that the particles are separated from the solution. However, other concerns may arise regarding the ionic dissociation of these particles in water. Jahan et al. [162] reported the dissociation and ionic metal loss of three coated MNPs through a column transport experiment, and the observed losses were between 1.6% and 19%. This ionic release behavior of some MNPs might affect the quality of produced water from the FO process since the dissociated ions would not be easily recovered. Thus, the released ions and/or monomers from MNPs adds another challenge that needs to be considered carefully before deploying MNPs in water treatment applications.

The potential utilization of iron oxide MNPs in water treatment mandates the exploration of how such nanomaterials are to be dealt with and the steps to be taken to avoid causing damage to the environment and human beings. Even though MNPs were approved for use in medicine and plentiful toxicity studies were carried out, the implementation of MNPs in water treatment applications still needs updated protocols of the current standards to promote human health and safety [167]. Any legislated regulations attaining the mitigation of threats pertaining to any substance would be established relying on the product type and amount. For example, although MNPs are not explicitly stipulated in the general obligations of REACH (Registration, Evaluation, Authorization and Restriction of Chemicals) for the European community, it is claimed that their regulations cover the safe and standard use of nanomaterials since it falls under the definition of “substance”. On the other hand, the Scientific Committee on Emerging and Newly Identified Health Risks (SCENIHR) stated that enhanced methods of assessment and instruments

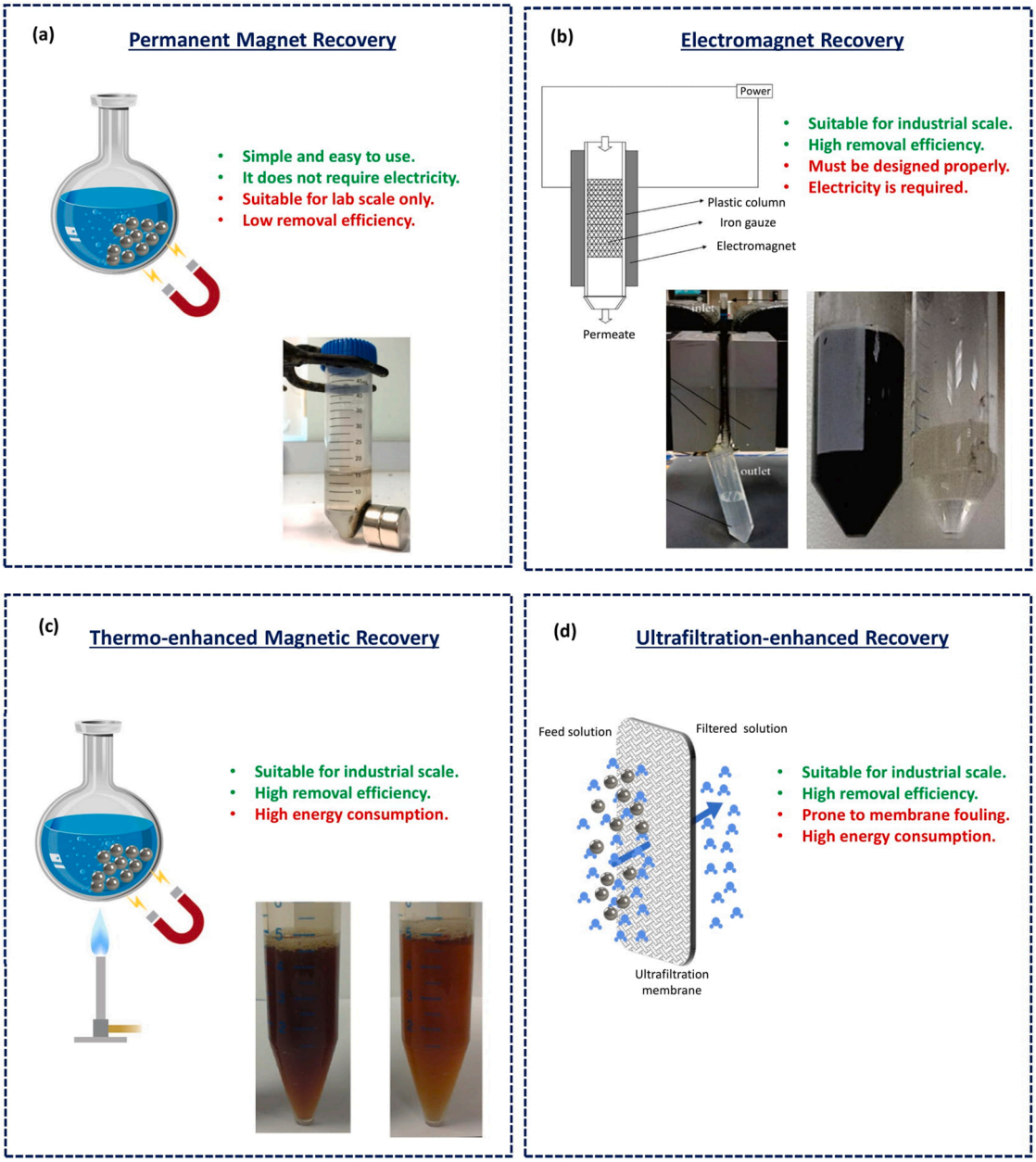

Fig. 8. Regeneration of MNPs after the dilution stage in the FO process: (a) permanent magnet recovery, citric acid coated MNPs using permanent magnet [114], (b) electromagnet recovery, diluted draw solution containing polyethylene glycol terminated with carboxylic group (left photo) [94], and recovered polyethylene glycol terminated with carboxylic group solution (right photo) [94]. (c) Thermo-sensitive MNPs coated with copolymer poly(sodium styrene-4-sulfonate)-co-poly (N-isopropylacrylamide), magnetic recovery without heat (left photo) [103], and enhanced magnetic recovery after heating the solution (right photo) [103], (d) enhanced recovery of MNPs using ultrafiltration after the magnetic recovery.

are still required when it comes to dealing with nano-sized materials. They believe that nanomaterials can exhibit various toxicological characteristics and case-by-case assessments must be employed. Furthermore, by checking other Water quality standards issued by environmental protection agencies and the Drinking-water quality guidelines issued by the world health organization, it can be said that the legal regulations governing the control and regulation of MNPs in water treatment still suffer from the lack of knowledge and understanding of the potential threats imposed by these materials. Therefore, extensive research is still needed on determining the toxicity of MNPs when taken orally, and more attention must be given by the legislators to overcome this challenge.

6. Concluding remarks and knowledge gaps

Forward osmosis could be the most sustainable membrane process for wastewater treatment and desalination due to low energy consumption and high resistance to fouling. However, extensive research is still needed to design a sustainable draw solute which can induce high osmotic pressure and easily retrieved from the diluted draw solution. In this review, we focused on the current status and challenges for using magnetic nanoparticles as a sustainable draw solute in the FO process. First, we highlighted the common synthesis methods of magnetic nanoparticles, and basics for generation of osmotic pressure using magnetic nanoparticles. Then, we studied the performance and limitations of the available MNPs that was used as draw solute in the FO process. Later, we assessed the toxicity level of the MNPs and the

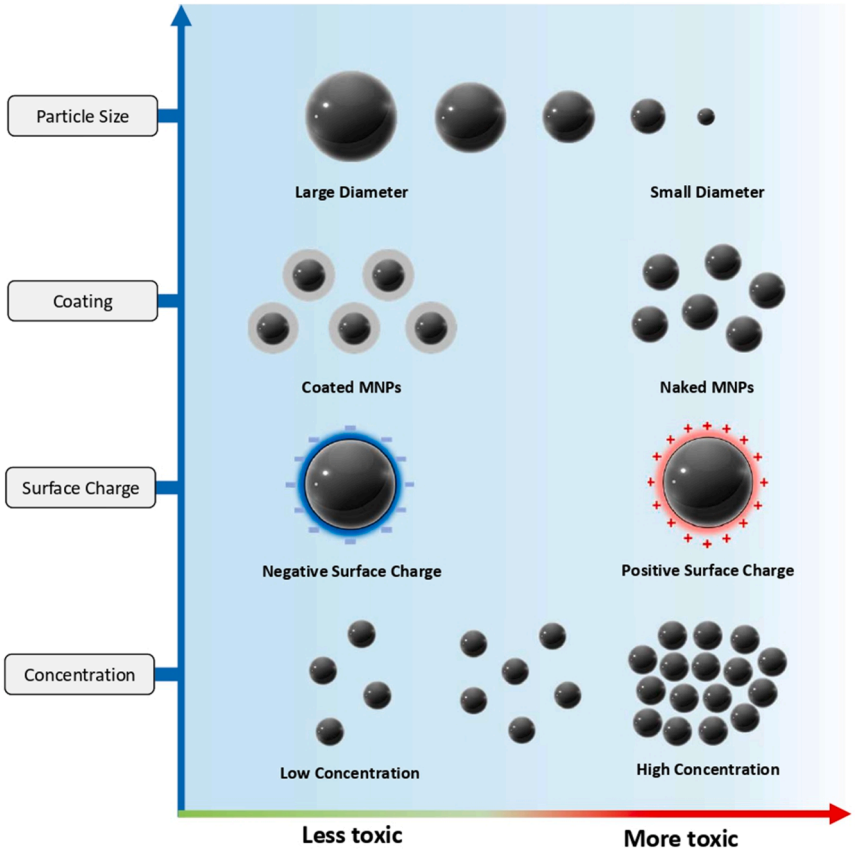

Fig. 9. The relationship between the properties of the MNPs and the toxicity level. It can be inferred that smaller MNPs are more toxic compared to smaller particles due to high penetration capabilities through the cell. The coated MNPs are less toxic compared to the bare MNPs due to the larger hydrated diameter and biocompatibility of the coating polymer.

regulations of using nanoparticles in water treatment industry. Based on the analysis in this study, the desired properties for an efficient MNPs draw solution have been recommended.

The efficient MNPs draw solute must generate high osmotic pressure and have the following characteristics: low reverse diffusion, high magnetic saturation, and low tendency for agglomeration. To achieve the aforementioned properties, various MNPs properties must be controlled such as particle size, shape, charge, hydrophilicity, and particles agglomeration. As can be inferred from the available literature, the optimum nanoparticle size must be controlled at an average size of (15–20 nm), this will generate high osmotic pressure due to the high surface-volume ratio. However, the particle size should not be less than 15 nm to inhibit the reverse diffusion of MNPs from the DS to FS, also to ensure full recovery using an external magnet. The particles must be negatively charged to prevent membrane fouling, because most of the FO membranes are negatively charged. Positively charged MNPs could accumulate on the membrane surface due to electrostatic attraction which causes irreversible membrane fouling. The MNPs must be highly hydrophilic, since the solubility of the nanoparticles increases as the hydrophilicity increase which results in higher osmotic pressure of the solution. Particle's agglomeration is the most challenging limitation where significant research is needed before solving this limitation. The particle's agglomeration can be inhibited by coating the MNPs using various coating agents, the coating agent must be selected based on the induced water flux and low level of toxicity. Various coating agents have been used to stabilize the MNPs used as a draw solute in the FO process, this includes natural polymers, synthetic polymers, and other non-polymeric coatings. Polyethylene glycol terminated with carboxylic group was found to be the most efficient coating to be used for the MNPs. This is due to the high water flux, low cost, and low toxicity. Nevertheless, the water flux obtained when using seawater or treated wastewater as feed solution was relatively low. Therefore, the most critical challenges and research gaps to be mitigated before implementing the technology efficiently for wastewater treatment and desalination are listed below:

- Develop a theoretical or a computational model to estimate the osmotic pressure created by the MNPs and the water flux in the forward osmosis process. This is due to the poor performance of the available equation and models in predicting the osmotic pressure generated by the MNPs. More research effort must be done on calculating the osmotic pressure created by coated MNPs using Donnan equilibrium equations.
- Evaluate the membrane fouling caused by MNPs by monitoring the process performance at an extended experimental time and using various types of coating agents for the MNPs. This is critical to prove the feasibility of the process since it affects operating cost of the process.

Table 3
Toxicity assessment of MNPs based on the coating agent and particle size of the particles.

Base material	Coating / Functional group	Particle size	Remarks about toxicity	Reference
Magnetite (Fe_3O_4)	Chitosan oligosaccharide	8 ± 2.7 nm (TEM)	• This test has aimed to assess the level of toxicity of coated MNPs by comparing them to bare iron oxide MNPs. The study outcomes have displayed reduced toxic effects of coated MNPs.	[158]
Maghemite (Fe_2O_3)	Polyethyleneimine Polyacrylic acid	12 nm (TEM) 28 – 30 nm (DLS)	• The potential toxicity of MNPs on pregnant mice based on the dosage and surface charge was assessed. The two concentrations used were 10 mg/kg and 100 mg/kg. • At the low dosage, regardless of the charge, no inherent toxicity of both MNPs was indicated. However, at the high concentration (100 mg/kg), fetal losses have incurred depending on the surface charge.	[163]
Magnetite (Fe_3O_4)	Chitosan	30–40 nm (TEM) 55 nm (DLS)	• Lab tests were performed on rat and human cells to evaluate MNPs toxicity using concentration of 1–150 μg/mL. • Chitosan coating has increased the surface charge of MNPs, which enhanced their inter-cellular uptake and thus became more toxic.	[159]
Magnetite (Fe_3O_4)	Ascorbate Citrate Dextran Polyvinylpyrrolidone	5 – 6 nm (TEM) 23 – 32 nm (DLS)	• The purpose of this study was to do a comparison between the produced toxicity on water flea caused by the different types of coating. The toxicity was investigated over 96 h and at concentrations of 0, 1, 2.5, 5, 7.5, 10, 25, 50, 75, and 100 mg-iron/L • Polyvinylpyrrolidone coated nanoparticles have shown the lowest toxicity compared to the remaining MNPs.	[164]
Maghemite (Fe_2O_3)	Polyethylene glycol	3 nm and 19 nm (TEM) 21 and 56 nm (DLS)	• Two particle sizes of PEG coated MNPs were tested on zebrafish embryos to assess their in vivo toxicity at concentrations of 1–100 μg/mL. • At the highest concentration (100 μg/mL) and an exposure duration of 48 h, both MNPs showed low toxicity and biocompatibility for in vivo MRI imaging as they accelerated the hatching rate and did not influence the survival rate of embryos.	[160]
Magnetite (Fe_3O_4)	Polyglycerol	6 – 9 nm (TEM) 24 ± 3 nm (DLS)	• The in vitro cytotoxicity of coated MNPs on fibroblasts and macrophages was investigated at the following concentrations: 25, 50, 100, and 200 μg/mL. • After 24 h of incubation, the cell viabilities were found to be not affected by the PG coated MNPs at all dosages, indicating no alarming toxicity levels.	[161]
Maghemite (Fe_2O_3)	Dimercaptosuccinic acid Citrate lauric acid	42 nm (DLS) 62 nm (DLS) 73 nm (DLS)	• In vitro testing for the listed MNPs was done on a human melanoma cell line. • The results demonstrated no cytotoxic responses of all MNPs at concentrations below 252 μg-iron/mL.	[165]
Magnetite (Fe_3O_4)	Chitosan Alginate	620 nm (TEM) 253 nm (TEM)	• The MNPs were examined using an in vitro cytotoxicity assay on kidney cells at a concentration of 26 μg/mL. and incubation times of 4 h and 24 h. • The tested MNPs showed no toxic impacts on the cultured cells.	[166]

- Evaluate the energy consumption and recovery efficiency for the regeneration of MNPs using electromagnets. The energy consumption of the magnetic regeneration process must be compared with the energy consumption of the other regeneration processes.
- Evaluate the economic feasibility for using MNPs as draw solute at a pilot scale forward osmosis process by comparing the capital cost and operating cost of the process with reverse osmosis since it is the most used membrane process for desalination and wastewater treatment.
- Regulations and standards for using MNPs in water treatment are missing from international standards. The available regulation and standards must specify the concentration limits for using MNPs in water treatment applications.

CRediT authorship contribution statement

MhdAmmar Hafiz: Conceptualization, Methodology, Data curation, Formal analysis, Writing – original draft. **Amani Hassanein**: Data curation, Formal analysis, Writing – original draft. **Mohammed Talhami**: Data curation, Formal analysis, Writing – original draft. **Maryam AL-Ejji:** Writing – review & editing. **Mohammad K. Hassan**: Writing – review & editing. **Alaa H. Hawari**: Supervision, Writing – review & editing.

Declaration of Competing Interest

The authors declare that they have no known competing financial interests or personal relationships that could have appeared to influence the work reported in this paper.

Data availability

No data was used for the research described in the article.

Acknowledgment

This research is made possible by graduate sponsorship research award (GSRA6–1-0509–19021) from Qatar National Research Fund (QNRF). Also, the authors would like to thank Qatar University for funding this project through Collaborative Grant (CG) - Cycle 05 – ID492. The statements made herein are solely the responsibility of the authors. Open access funding was provided by Qatar National Library.

References

[1] J. Kim, K. Park, D.R. Yang, S. Hong, A comprehensive review of energy consumption of seawater reverse osmosis desalination plants, Appl. Energy 254 (2019), 113652.
[2] A. Matin, F. Rahman, H.Z. Shafi, S.M. Zubair, Scaling of reverse osmosis membranes used in water desalination: Phenomena, impact, and control; future directions, Desalination 455 (2019) 135–157.
[3] A. Matin, T. Laoui, W. Falath, M. Farooque, Fouling control in reverse osmosis for water desalination & reuse: Current practices & emerging environment-friendly technologies, Sci. Total Environ. 765 (2020), 142721.
[4] Y.-N. Wang, K. Goh, X. Li, L. Setiawan, R. Wang, Membranes and processes for forward osmosis-based desalination: Recent advances and future prospects, Desalination 434 (2018) 81–99.
[5] L. Li, X.-p Liu, H.-q Li, A review of forward osmosis membrane fouling: types, research methods and future prospects, Environ. Technol. Rev. 6 (1) (2017) 26–46.
[6] R. Alfahel, R.S. Azzam, M. Hafiz, A.H. Hawari, R.P. Pandey, K.A. Mahmoud, M. K. Hassan, A.A. Elzatahry, Fabrication of fouling resistant Ti3C2Tx (MXene)/ cellulose acetate nanocomposite membrane for forward osmosis application, J. Water Process Eng. 38 (2020), 101551.
[7] M.A. Hafiz, A.H. Hawari, A. Altaee, A hybrid forward osmosis/reverse osmosis process for the supply of fertilizing solution from treated wastewater, J. Water Process Eng. 32 (2019), 100975.
[8] M. Pejman, M.D. Firouzjaei, S.A. Aktij, P. Das, E. Zolghadr, H. Jafarian, A. A. Shamsabadi, M. Elliott, M.R. Esfahani, M. Sangermano, M. Sadrzadeh, E. K. Wujcik, A. Rahimpour, A. Tiraferri, Improved antifouling and antibacterial properties of forward osmosis membranes through surface modification with zwitterions and silver-based metal organic frameworks, J. Membr. Sci. 611 (2020), 118352.
[9] Y. Yabuno, K. Mihara, N. Miyagawa, K. Komatsu, K. Nakagawa, T. Shintani, H. Matsuyama, T. Yoshioka, Preparation of polyamide–PVDF composite hollow fiber membranes with well-developed interconnected bicontinuous structure

using high-temperature rapid NIPS for forward osmosis, J. Membr. Sci. 612 (2020), 118468.
[10] W. Wu, Y. Shi, G. Liu, X. Fan, Y. Yu, Recent development of graphene oxide based forward osmosis membrane for water treatment: A critical review, Desalination 491 (2020), 114452.
[11] M.S. Thabit, A.H. Hawari, M.H. Ammar, S. Zaidi, G. Zaragoza, A. Altaee, Evaluation of forward osmosis as a pretreatment process for multi stage flash seawater desalination, Desalination 461 (2019) 22–29.
[12] A.J. Ansari, F.I. Hai, W.E. Price, J.E. Drewes, L.D. Nghiem, Forward osmosis as a platform for resource recovery from municipal wastewater - A critical assessment of the literature, J. Membr. Sci. 529 (2017) 195–206.
[13] G. Blandin, et al., Oppor. Reach Econ. Sustain. Forw. osmosis–reverse osmosis hybrids Seawater Desalin. 363 (2015) 26–36.
[14] M. Xie, L.D. Nghiem, W.E. Price, M. Elimelech, Comparison of the removal of hydrophobic trace organic contaminants by forward osmosis and reverse osmosis, Water Res. 46 (8) (2012) 2683–2692.
[15] H.T. Nguyen, N.C. Nguyen, S.S. Chen, H.H. Ngo, W. Guo, C.W. Li, A new class of draw solutions for minimizing reverse salt flux to improve forward osmosis desalination, Sci. Total Environ. 538 (2015) 129–136.
[16] P. Zhao, B. Gao, Q. Yue, J. Kong, H.K. Shon, P. Liu, Y. Gao, Explore the forward osmosis performance using hydrolyzed polyacrylamide as draw solute for dye wastewater reclamation in the long-term process, Chem. Eng. J. 273 (2015) 316–324.
[17] Q. Ge, J. Su, G.L. Amy, T.S. Chung, Exploration of polyelectrolytes as draw solutes in forward osmosis processes, Water Res. 46 (4) (2012) 1318–1326.
[18] D. Zhao, P. Wang, Q. Zhao, N. Chen, X. Lu, Thermoresponsive copolymer-based draw solution for seawater desalination in a combined process of forward osmosis and membrane distillation, Desalination 348 (2014) 26–32.
[19] N.T. Hau, S.S. Chen, N.C. Nguyen, K.Z. Huang, H.H. Ngo, W. Guo, Exploration of EDTA sodium salt as novel draw solution in forward osmosis process for dewatering of high nutrient sludge, J. Membr. Sci. 455 (2014) 305–311.
[20] E. Tian, C. Hu, Y. Qin, Y. Ren, X. Wang, X. Wang, P. Xiao, X. Yang, A study of poly (sodium 4-styrenesulfonate) as draw solute in forward osmosis, Desalination 360 (2015) 130–137.
[21] T. Hu, X. Wang, C. Wang, X. Li, Y. Ren, Impacts of inorganic draw solutes on the performance of thin-film composite forward osmosis membrane in a microfiltration assisted anaerobic osmotic membrane bioreactor, RSC Adv. 7 (26) (2017) 16057–16063.
[22] A. Achilli, T. Cath, A. Childress, Selection of inorganic-based draw solutions for forward osmosis applications, J. Membr. SCI. - J. Membr. SCI 364 (2010) 233–241.
[23] D. Roy, M. Rahni, P. Pierre, V. Yargeau, Forward osmosis for the concentration and reuse of process saline wastewater, Chem. Eng. J. 287 (2016) 277–284.
[24] S. Phuntsho, H.K. Shon, S. Hong, S. Lee, S. Vigneswaran, J. Kandasamy, Fertiliser drawn forward osmosis desalination: the concept, performance and limitations for fertigation, Rev. Environ. Sci. Bio/Technol. 11 (2) (2012) 147–168.
[25] Y. Oh, S. Lee, M. Elimelech, S. Lee, S. Hong, Effect of hydraulic pressure and membrane orientation on water flux and reverse solute flux in pressure assisted osmosis, J. Membr. Sci. 465 (2014) 159–166.
[26] J.R. McCutcheon, R.L. McGinnis, M. Elimelech, A novel ammonia—carbon dioxide forward (direct) osmosis desalination process, Desalination 174 (1) (2005) 1–11.
[27] M.L. Stone, C. Rae, F.F. Stewart, A.D. Wilson, Switchable polarity solvents as draw solutes for forward osmosis, Desalination 312 (2013) 124–129.
[28] T. Alejo, M. Arruebo, V. Carcelen, V.M. Monsalvo, V. Sebastian, Advances in draw solutes for forward osmosis: Hybrid organic-inorganic nanoparticles and conventional solutes, Chem. Eng. J. 309 (2017) 738–752.
[29] J. Wang, X. Liu, Forward osmosis technology for water treatment: Recent advances and future perspectives, J. Clean. Prod. 280 (2021), 124354.
[30] H. Luo, Q. Wang, T.C. Zhang, T. Tao, A. Zhou, L. Chen, X. Bie, A review on the recovery methods of draw solutes in forward osmosis, J. Water Process Eng. 4 (2014) 212–223.
[31] M. Puppala, X. Zhao, D. Casemore, B. Zhou, G. Aridoss, S. Narayanapillai, C. Xing, Multi-functional forward osmosis draw solutes for seawater desalination, Chin. J. Chem. Eng. 24 (1) (2016) 23–30.
[32] D.J. Johnson, W.A. Suwaileh, A.W. Mohammed, N. Hilal, Osmotic's potential: An overview of draw solutes for forward osmosis, Desalination 434 (2018) 100–120.
[33] M.J.A. Hamad, E.M.N. Chirwa, Forward osmosis for water recovery using polyelectrolyte PolyDADMAC and DADMAC draw solutions as a low pressure energy saving process, Desalination 453 (2019) 89–101.
[34] I. Fatimah, G. Fadillah, S.P. Yudha, Synthesis of iron-based magnetic nanocomposites: A review, Arab. J. Chem. 14 (8) (2021), 103301.
[35] U. Schwertmann, R.M. Cornell, Iron Oxides in the Laboratary, Iron oxides Lab.: Prep. Charact. (2000).
[36] W. Wu, Q. He, C. Jiang, Magnetic iron oxide nanoparticles: synthesis and surface functionalization strategies, Nanoscale Res. Lett. 3 (11) (2008) 397–415.
[37] A.S. Teja, P.-Y. Koh, Synthesis, properties, and applications of magnetic iron oxide nanoparticles, Prog. Cryst. Growth Charact. Mater. 55 (1) (2009) 22–45.
[38] X. Peng, J. Ding, Y. Feng, in: R. Lucena, S. Cárdenas (Eds.), *12 - Metal and metal oxide nanomaterials in sample preparation*, in *Analytical Sample Preparation With Nano- and Other High-Performance Materials*, Elsevier, 2021, pp. 297–322.
[39] R. Nisticò, A synthetic guide toward the tailored production of magnetic iron oxide nanoparticles, Bol. De. la Soc. Esp. De. Cerámica Y. Vidr. 60 (1) (2021) 29–40.
[40] F.E. Kruis, H. Fissan, A. Peled, Synthesis of nanoparticles in the gas phase for electronic, optical and magnetic applications—a review, J. Aerosol Sci. 29 (5) (1998) 511–535.
[41] P. Liu, W. Cai, H. Zeng, *Fabrication and Size-Dependent Optical Properties of FeO Nanoparticles Induced by Laser Ablation in a Liquid Medium.* The, J. Phys. Chem. C. 112 (9) (2008) 3261–3266.
[42] V. Amendola, M. Meneghetti, Laser ablation synthesis in solution and size manipulation of noble metal nanoparticles, Phys. Chem. Chem. Phys. 11 (20) (2009) 3805–3821.
[43] M.K. Corbierre, J. Beerens, R.B. Lennox, Gold Nanoparticles Generated by Electron Beam Lithography of Gold(I)−Thiolate Thin Films, Chem. Mater. 17 (23) (2005) 5774–5779.
[44] R. Arbain, M. Othman, S. Palaniandy, Preparation of iron oxide nanoparticles by mechanical milling, Miner. Eng. 24 (1) (2011) 1–9.
[45] S. Veintemillas-Verdaguer, M.P. Morales, C.J. Serna, Continuous production of γ-Fe2O3 ultrafine powders by laser pyrolysis, Mater. Lett. 35 (3) (1998) 227–231.
[46] S. Yang, Y.H. Jang, C.H. Kim, C. Hwang, J. Lee, S. Chae, S. Jung, M. Choi, A flame metal combustion method for production of nanoparticles, Powder Technol. 197 (3) (2010) 170–176.
[47] A.-G. Niculescu, C. Chircov, A.M. Grumezescu, Magnetite nanoparticles: Synthesis methods – A comparative review, Methods 199 (2021) 16–27.
[48] A.P. LaGrow, M.O. Besenhard, A. Hodzic, A. Sergides, L.K. Bogart, A. Gavriilidis, N. Thanh, Unravelling the growth mechanism of the co-precipitation of iron oxide nanoparticles with the aid of synchrotron X-Ray diffraction in solution, Nanoscale 11 (14) (2019) 6620–6628.
[49] A. Lassenberger, T.A. Grünewald, P. van Oostrum, H. Rennhofer, H. Amenitsch, R. Zirbs, H.C. Lichtenegger, E. Reimhult, Monodisperse Iron Oxide Nanoparticles by Thermal Decomposition: Elucidating Particle Formation by Second-Resolved in Situ Small-Angle X-ray Scattering, Chem. Mater. 29 (10) (2017) 4511–4522.
[50] T.J. Daou, G. Pourroy, S. Bégin-Colin, J.M. Grenèche, C. Ulhaq-Bouillet, P. Legaré, P. Bernhardt, C. Leuvrey, G. Rogez, Hydrothermal synthesis of monodisperse magnetite nanoparticles, Chem. Mater. 18 (18) (2006) 4399–4404.
[51] K. Kekalo, K. Koo, E. Zeitchick, I. Baker, *Mic*roemulsi*on* synthesis of iron core/iron oxide shell magnetic nanoparticles and their physicochemical pro*perties*, Mater. Res. Soc. Symp. Proc. Mater. Res. Soc. 1416 (2012) 10, 1557/opl.2012.736.
[52] M. Nawaz, et al., in: A.S.H. Makhlouf, N.Y. Abu-Thabit (Eds.), *2 - Magnetic and pH-responsive magnetic nanocarriers*, in *Stimuli Responsive Polymeric Nanocarriers for Drug Delivery Applications*, Woodhead Publishing, 2019, pp. 37–85.
[53] J.S. Beveridge, J.R. Stephens, M.E. Williams, The use of magnetic nanoparticles in analytical chemistry, Annu Rev. Anal. Chem. (Palo Alto Calif.) 4 (2011) 251–273.
[54] C. Ravikumar, R. Bandyopadhyaya, *Mechanistic study on magnetite nanoparticle formation by thermal decomposition and coprecipitation routes*, J. Phys. Chem. C. 115 (5) (2011) 1380–1387.
[55] N.T.K. Thanh, N. Maclean, S. Mahiddine, Mechanisms of nucleation and growth of nanoparticles in solution, Chem. Rev. 114 (15) (2014) 7610–7630.
[56] T. Athar, in: W. Ahmed, M.J. Jackson (Eds.), *Chapter 17 - Smart precursors for smart nanoparticles*, in *Emerging Nanotechnologies for Manufacturing, Second edition.*,, William Andrew Publishing, Boston, 2015, pp. 444–538.
[57] L.S. Ganapathe, et al., Magn. (Fe3O4) Nanopart. Biomed. Appl.: Synth. Surf. Funct. 6 (4) (2020) 68.
[58] G. Huang, C.-H. Lu, H.-H. Yang, *Magnetic nanomaterials for magnetic bioanalysis*, in *Novel Nanomaterials for Biomedical*. Environmental and Energy Applications, Elsevier,, 2019, pp. 89–109.
[59] S. Kalia, S. Kango, A. Kumar, Y. Haldorai, B. Kumari, R. Kumar, Magnetic polymer nanocomposites for environmental and biomedical applications, Colloid Polym. Sci. 292 (9) (2014) 2025–2052.
[60] T. Ahn, J.H. Kim, H.M. Yang, J.W. Lee, J.D. Kim, *Formation Pathways of Magnetite Nanoparticles by Coprecipitation Method.* The, J. Phys. Chem. C. 116 (10) (2012) 6069–6076.
[61] Freitas, D.A., Paiva A.L., Carvalho Filho J.A., Cabral J.J., Rocha F.J., Occurrence of Cryptosporidium spp., Giardia spp. and other pathogenic intestinal parasites in the Beberibe River in the State of Pernambuco, Brazil, Magnetic nanoparticles obtained by homogeneous coprecipitation sonochemically assisted. 2015. 18: p. 220–224.
[62] S. Majidi, F.Z. Sehrig, S.M. Farkhani, M.S. Goloujeh, A. Akbarzadeh, Current methods for synthesis of magnetic nanoparticles, Artif. Cells, Nanomed., Biotechnol. 44 (2) (2016) 722–734.
[63] H. Iida, K. Takayanagi, T. Nakanishi, T. Osaka, Synthesis of Fe3O4 nanoparticles with various sizes and magnetic properties by controlled hydrolysis, J. Colloid Interface Sci. 314 (1) (2007) 274–280.
[64] J.-H. Kim, S.-M. Kim, Y.-I. Kim, Properties of magnetic nanoparticles prepared by co-precipitation, J. Nanosci. Nanotechnol. 14 (2014) 14–8744.
[65] M.I. Khalil, Co-precipitation in aqueous solution synthesis of magnetite nanoparticles using iron(III) salts as precursors, Arab. J. Chem. 8 (2) (2015) 279–284.
[66] H. Ke, W. Wang, Y. Wang, J. Xu, D. Jia, Z. Lu, Y. Zhou, Factors controlling pure-phase multiferroic BiFeO3 powders synthesized by chemical co-precipitation, J. Alloy. Compd. 509 (5) (2011) 2192–2197.
[67] A.-H. Lu, E.L. Salabas, F. Schüth, Magnetic nanoparticles: synthesis, protection, functionalization, and application, Angew. Chem. Int. Ed. 46 (8) (2007) 1222–1244.
[68] A. Figuerola, R. Di Corato, L. Manna, T. Pellegrino, From iron oxide nanoparticles towards advanced iron-based inorganic materials designed for biomedical applications, Pharmacol. Res. 62 (2) (2010) 126–143.

[69] C.-h Chia, et al., Size-controlled Synthesis and Characterization of Fe3O4 Nanoparticles by Chemical Coprecipitation Method, Sains Malays. (2008) **37**.
[70] N.D. Kandpal, et al., Co-precipitation method of synthesis and characterization of iron oxide nanoparticles, J. Sci. Ind. Res. 73 (2014) 87–90.
[71] S.-J. Lee, J.R. Jeong, S.C. Shin, J.C. Kim, J.D. Kim, Synthesis and characterization of superparamagnetic maghemite nanoparticles prepared by coprecipitation technique, J. Magn. Magn. Mater. 282 (2004) 147–150.
[72] J.-R. Jeong, et al., Magn. Prop. γ-Fe2O3 Nanopart. made coprecipitation Method 241 (7) (2004) 1593–1596.
[73] R. Hao, R. Xing, Z. Xu, Y. Hou, S. Gao, S. Sun, Synthesis, functionalization, and biomedical applications of multifunctional magnetic nanoparticles, Adv. Mater. 22 (25) (2010) 2729–2742.
[74] T. Hyeon, S.S. Lee, J. Park, Y. Chung, H.B. Na, Synthesis of highly crystalline and monodisperse maghemite nanocrystallites without a size-selection process, J. Am. Chem. Soc. 123 (51) (2001) 12798–12801.
[75] Z. Xu, C. Shen, Y. Tian, X. Shi, H.J. Gao, Organic phase synthesis of monodisperse iron oxide nanocrystals using iron chloride as precursor, Nanoscale 2 (6) (2010) 1027–1032.
[76] A.-G. Niculescu, C. Chircov, A.M. Grumezescu, Magnetite nanoparticles: Synthesis methods – A comparative review, Methods 199 (2022) 16–27.
[77] S. Chin, S. Pang, C.-H. Tan, Green Synthesis of Magnetite Nanoparticles (via Thermal Decomposition Method) with Controllable Size and Shape, J. Mater. Environ. Sci. (2011) **2**.
[78] W.W. Yu, J.C. Falkner, C.T. Yavuz, V.L. Colvin, Synthesis of monodisperse iron oxide nanocrystals by thermal decomposition of iron carboxylate salts, Chem. Commun. 20 (2004) 2306–2307.
[79] Yang, F., et al., Bioimaging: An Integrated Multifunctional Nanoplatform for Deep-Tissue Dual-Mode Imaging (Adv. Funct. Mater. 11/2018), 2018. 28(11): p. 1870073.
[80] J.R. Sosa-Acosta, C. Iriarte-Mesa, G.A. Ortega, A.M. Díaz-García, DNA–iron oxide nanoparticles conjugates: functional magnetic nanoplatforms in biomedical applications, Top. Curr. Chem. 378 (1) (2020) 13.
[81] C. Pereira, A.M. Pereira, C. Fernandes, M. Rocha, R. Mendes, M.P. Fernández-García, A. Guedes, P.B. Tavares, J.M. Grenèche, J.P. Araújo, C. Freire, Superparamagnetic MFe2O4 (M = Fe, Co, Mn) Nanoparticles: Tuning the Particle Size and Magnetic Properties through a Novel One-Step Coprecipitation Route, Chem. Mater. 24 (8) (2012) 1496–1504.
[82] Colligative Properties - Osmotic Pressure, 2021.
[83] A. Philipse, A. Vrij, The Donnan equilibrium: I. On the thermodynamic foundation of the Donnan equation of state, J. Phys.: Condens. Matter 23 (19) (2011), 194106.
[84] J.-M.Y. Carrillo, A.V. Dobrynin, Salt Effect on Osmotic Pressure of Polyelectrolyte Solutions: Simulation Study, Polymers 6 (7) (2014) 1897–1913.
[85] D.J. Winzor, Reappraisal of disparities between osmolality estimates by freezing point depression and vapor pressure deficit methods, Biophys. Chem. 107 (3) (2004) 317–323.
[86] M. Guizani, T. Maeda, R. Ito, N. Funamizu, Synthesis and Characterization of Magnetic Nanoparticles as a Candidate Draw Solution for Forward Osmosis, J. Water Environ. Technol. 16 (1) (2018) 63–71.
[87] X. Guo, Z. Wu, W. Li, Z. Wang, Q. Li, F. Kong, H. Zhang, X. Zhu, Y.P. Du, Y. Jin, Y. Du, J. You, Appropriate size of magnetic nanoparticles for various bioapplications in cancer diagnostics and therapy, ACS Appl. Mater. Interfaces 8 (5) (2016) 3092–3106.
[88] H. Heinz, C. Pramanik, O. Heinz, Y. Ding, R.K. Mishra, D. Marchon, R.J. Flatt, I. Estrela-Lopis, J. Llop, S. Moya, R.F. Ziolo, Nanoparticle decoration with surfactants: Molecular interactions, assembly, and applications, Surf. Sci. Rep. 72 (1) (2017) 1–58.
[89] A.M. El Badawy, T.P. Luxton, R.G. Silva, K.G. Scheckel, M.T. Suidan, T. M. Tolaymat, Impact of Environmental Conditions (pH, Ionic Strength, and Electrolyte Type) on the Surface Charge and Aggregation of Silver Nanoparticles Suspensions, Environ. Sci. Technol. 44 (4) (2010) 1260–1266.
[90] S. Zhao, L. Zou, D. Mulcahy, Effects of membrane orientation on process performance in forward osmosis applications, J. Membr. Sci. 382 (1) (2011) 308–315.
[91] R. Honda, W. Rukapan, H. Komura, Y. Teraoka, M. Noguchi, E.M. Hoek, Effects of membrane orientation on fouling characteristics of forward osmosis membrane in concentration of microalgae culture, Bioresour. Technol. 197 (2015) 429–433.
[92] A. Tayel, P. Nasr, H. Sewilam, Enhanced water flux using uncoated magnetic nanoparticles as a draw solution in forward osmosis desalination, Desalin. Water Treat. 193 (2020) 169–176.
[93] Hafiz, M., et al., Optimization of Magnetic Nanoparticles Draw Solution for High Water Flux in Forward Osmosis, 2021: 13(24): p. 3653.
[94] Q. Ge, et al., Hydrophilic superparamagnetic nanoparticles: synthesis, characterization, and performance in forward osmosis processes, Ind. Eng. Chem. Res. 50 (1) (2011) 382–388.
[95] M. Guizani, et al., Polyethylene glycol-coated magnetic nanoparticles-based draw solution for forward osmosis, Sanit. Value Chain 4 (1) (2020) 27–37.
[96] T. Mishra, S. Ramola, A.K. Shankhwar, R.K. Srivastava, Use of synthesized hydrophilic magnetic nanoparticles (HMNPs) in forward osmosis for water reuse, Water Supply 16 (1) (2015) 229–236.
[97] Y. Xue, J. Lee, H.J. Kim, H.J. Cho, X. Zhou, Y. Liu, P. Tebon, T. Hoffman, M. Qu, H. Ling, X. Jiang, Z. Li, S. Zhang, W. Sun, S. Ahadian, M.R. Dokmeci, K. Lee, A. Khademhosseini, Highly stable superparamagnetic iron oxide nanoparticles as functional draw solutes for osmotically driven water transport, npj Clean. Water 3 (1) (2020) 8–6918.
[98] M.M. Ling, T.-S. Chung, Novel dual-stage FO system for sustainable protein enrichment using nanoparticles as intermediate draw solutes, J. Membr. Sci. 372 (1) (2011) 201–209.
[99] J. Zufía-Rivas, P. Morales, S. Veintemillas-Verdaguer, Effect of the Sodium Polyacrylate on the Magnetite Nanoparticles Produced by Green Chemistry Routes: Applicability in Forward Osmosis, Nanomaterials 8 (2018) 470.
[100] Ban, I., et al., Synthesis of Poly-Sodium-Acrylate (PSA)-Coated Magnetic Nanoparticles for Use in Forward Osmosis Draw Solutions, 2019: 9(9): p. 1238.
[101] M. Joafshan, A. Shakeri, S.R. Razavi, H. Salehi, Gas responsive magnetic nanoparticle as novel draw agent for removal of Rhodamine B via forward osmosis: High water flux and easy regeneration, Sep. Purif. Technol. 282 (2022), 119998.
[102] A. Zhou, H. Luo, Q. Wang, L. Chen, T.C. Zhang, T. Tao, Magnetic thermoresponsive ionic nanogels as novel draw agents in forward osmosis, RSC Adv. 5 (20) (2015) 15359–15365.
[103] Q. Zhao, N. Chen, D. Zhao, X. Lu, Thermoresponsive magnetic nanoparticles for seawater desalination, ACS Appl. Mater. Interfaces 5 (21) (2013) 11453–11461.
[104] Z. Shabani, A. Rahimpour, Chitosan- and dehydroascorbic acid-coated Fe3O4 nanoparticles: preparation, characterization and their potential as draw solute in forward osmosis process, Iran. Polym. J. 25 (2016) **25**–895.
[105] M.M. Ling, T.-S. Chung, X. Lu, Facile synthesis of thermosensitive magnetic nanoparticles as "smart" draw solutes in forward osmosis, Chem. Commun. 47 (38) (2011) 10788–10790.
[106] M.M. Ling, K.Y. Wang, T.-S. Chung, Highly water-soluble magnetic nanoparticles as novel draw solutes in forward osmosis for water reuse, Ind. Eng. Chem. Res. 49 (12) (2010) 5869–5876.
[107] M.M. Ling, T.-S. Chung, Desalination process using super hydrophilic nanoparticles via forward osmosis integrated with ultrafiltration regeneration, Desalination 278 (1) (2011) 194–202.
[108] A. Shakeri, H. Salehi, N. Khankeshipour, M.T. Nakhjiri, F. Ghorbani, Magnetic nanoparticle-crosslinked ferrohydrogel as a novel class of forward osmosis draw agent, J. Nanopart. Res. 20 (12) (2018) 325.
[109] H. Bai, Z. Liu, D.D. Sun, Highly water soluble and recovered dextran coated Fe3O4 magnetic nanoparticles for brackish water desalination, Sep. Purif. Technol. 81 (3) (2011) 392–399.
[110] O.A. Attallah, M.A. Al-Ghobashy, M. Nebsen, R. El-Kholy, M.Y. Salem, Assessment of pectin-coated magnetite nanoparticles in low-energy water desalination applications, Environ. Sci. Pollut. Res. 25 (19) (2018) 18476–18483.
[111] F. Azadi, A. Karimi-Jashni, M.M. Zerafat, Desalination of brackish water by gelatin-coated magnetite nanoparticles as a novel draw solute in forward osmosis process, Environ. Technol. (2020) 1–11.
[112] F. Khazaie, S. Shokrollahzadeh, Y. Bide, S. Sheshmani, A.S. Shahvelayati, Forward osmosis using highly water dispersible sodium alginate sulfate coated-Fe3O4 nanoparticles as innovative draw solution for water desalination, Process Saf. Environ. Prot. 146 (2021) 789–799.
[113] Y. Na, S. Yang, S. Lee, Evaluation of citrate-coated magnetic nanoparticles as draw solute for forward osmosis, Desalination 347 (2014) 34–42.
[114] Q. Ge, L. Yang, J. Cai, W. Xu, Q. Chen, M. Liu, Hydroacid magnetic nanoparticles in forward osmosis for seawater desalination and efficient regeneration via integrated magnetic and membrane separations, J. Membr. Sci. 520 (2016) 550–559.
[115] K. Mylkie, et al., Polym. -Coat. Magn. Nanopart. Protein Immobil. 14 (2) (2021) 248.
[116] L.M. Sanchez, D.A. Martin, V.A. Alvarez, J.S. Gonzalez, Polyacrylic acid-coated iron oxide magnetic nanoparticles: The polymer molecular weight influence, Colloids Surf. A: Physicochem. Eng. Asp. 543 (2018) 28–37.
[117] T. Mishra, S. Ramola, A.K. Shankhwar, R.K. Srivastava, Use of synthesized hydrophilic magnetic nanoparticles (HMNPs) in forward osmosis for water reuse, Water Sci. Technol.: Water Supply 16 (2016) 229–236.
[118] H.-M. Yang, H.M. Choi, S.C. Jang, M.J. Han, B.K. Seo, J.K. Moon, K.W. Lee, Succinate functionalization of hyperbranched polyglycerol-coated magnetic nanoparticles as a draw solute during forward osmosis, J. Nanosci. Nanotechnol. 15 (2015) **15**–84.
[119] H.-M. Yang, C.W. Park, M.J. Han, B.K. Seo, J.K. Moon, K.W. Lee, Hyperbranched Polyglycerol Carboxylate-Coated Magnetic Nanoparticles as a Draw Solute in a Combined Forward Osmosis and Ultrafiltration Process, J. Nanosci. Nanotechnol. 16 (2016) 10858–10863.
[120] L. Arens, D. Barther, J. Landsgesell, C. Holm, M. Wilhelm, Poly(sodium acrylate) hydrogels: synthesis of various network architectures, local molecular dynamics, salt partitioning, desalination and simulation, Soft Matter 15 (48) (2019) 9949–9964.
[121] A. Shakeri, M.T. Nakhjiri, H. Salehi, F. Ghorbani, N. Khankeshipour, Preparation of polymer-carbon nanotubes composite hydrogel and its application as forward osmosis draw agent, J. Water Process Eng. 24 (2018) 42–48.
[122] A. Razmjou, Q. Liu, G.P. Simon, H. Wang, Bifunctional Polymer Hydrogel Layers As Forward Osmosis Draw Agents for Continuous Production of Fresh Water Using Solar Energy, Environ. Sci. Technol. 47 (22) (2013) 13160–13166.
[123] H. Liu, C. Wang, Q. Gao, J. Chen, B. Ren, X. Liu, Z. Tong, Facile fabrication of well-defined hydrogel beads with magnetic nanocomposite shells, Int. J. Pharm. 376 (1) (2009) 92–98.
[124] R. Barbucci, D. Pasqui, G. Giani, M. De Cagna, M. Fini, R. Giardino, A. Atrei, A novel strategy for engineering hydrogels with ferromagnetic nanoparticles as crosslinkers of the polymer chains. Potential applications as a targeted drug delivery system, Soft Matter 7 (12) (2011) 5558–5565.
[125] A.G.J. Voragen, G.J. Coenen, R.P. Verhoef, H.A. Schols, Pectin, a versatile polysaccharide present in plant cell walls, Struct. Chem. 20 (2) (2009) 263–275.

[126] A. Tayel, P. Nasr, H. Sewilam, Forward osmosis desalination using pectin-coated magnetic nanoparticles as a draw solution, Clean. Technol. Environ. Policy 21 (8) (2019) 1617–1628.
[127] D.D. Ngobeni, Removal of Manganese(II) Ion from Wastewater Using Low Cost Adsorbents and Exploration of the Reuse of the Manganese-Loaded Adsorbent in the Sensing of Volatile Organic Compounds, , University of Johannesburg (South Africa),, Ann Arbor, 2019, p. 124.
[128] F. Sharifianjazi, M. Irani, A. Esmaeilkhanian, L. Bazli, M.S. Asl, H.W. Jang, S. Y. Kim, S. Ramakrishna, M. Shokouhimehr, R.S. Varma, Polymer incorporated magnetic nanoparticles: Applications for magnetoresponsive targeted drug delivery, Mater. Sci. Eng.: B 272 (2021), 115358.
[129] I.O. Wulandari, V.T. Mardila, D.J.D.H. Santjojo, A. Sabarudin, Preparation and Characterization of Chitosan-coated Fe3O4 Nanoparticles using Ex-Situ Co-Precipitation Method and Tripolyphosphate/Sulphate as Dual Crosslinkers, IOP Conf. Ser.: Mater. Sci. Eng. 299 (2018), 012064.
[130] Z. Shabani, A. Rahimpour, Chitosan- and dehydroascorbic acid-coated Fe3O4 nanoparticles: preparation, characterization and their potential as draw solute in forward osmosis process, Iran. Polym. J. 25 (10) (2016) 887–895.
[131] N. Parikh, K. Parekh, Technique to optimize magnetic response of gelatin coated magnetic nanoparticles, J. Mater. Sci.: Mater. Med. 26 (7) (2015) 202.
[132] A.J. Szalai, N. Manivannan, G. Kaptay, Super-paramagnetic magnetite nanoparticles obtained by different synthesis and separation methods stabilized by biocompatible coatings, Colloids Surf. A: Physicochem. Eng. Asp. 568 (2019) 113–122.
[133] M. Razia, U. Nallal, S. Sivaramakrishnan, Agro-Based Sugarcane Ind. Wastes Prod. High. -Value Bioprod. (2020) 303–316.
[134] M. Mounir, et al., Ferric hydroacid & diamine complex as draw solute for forward osmosis (FO) desalination processes, Clean. Eng. Technol. 5 (2021), 100316.
[135] X.Y. Chi, P.Y. Zhang, X.J. Guo, Z.L. Xu, Interforce initiated by magnetic nanoparticles for reducing internal concentration polarization in CTA forward osmosis membrane, J. Appl. Polym. Sci. 134 (2017) 25.
[136] Z. Jiang, K. Shan, J. Song, J. Liu, S. Rajendran, A. Pugazhendhi, J.A. Jacob, B. Chen, Toxic effects of magnetic nanoparticles on normal cells and organs, Life Sci. 220 (2019) 156–161.
[137] N. Tran, T.J. Webster, Magnetic nanoparticles: biomedical applications and challenges, J. Mater. Chem. 20 (40) (2010) 8760–8767.
[138] Y.C. Sharma, V. Srivastava, V.K. Singh, S.N. Kaul, C.H. Weng, Nano-adsorbents for the removal of metallic pollutants from water and wastewater, Environ. Technol. 30 (6) (2009) 583–609.
[139] V. Srivastava, D. Gusain, Y.C. Sharma, Critical review on the toxicity of some widely used engineered nanoparticles, Ind. Eng. Chem. Res. 54 (24) (2015) 6209–6233.
[140] G. Oberdörster, E. Oberdörster, J. Oberdörster, Nanotoxicology: an emerging discipline evolving from studies of ultrafine particles, Environ. Health Perspect. 113 (7) (2005) 823–839.
[141] Z. Chen, H. Meng, G. Xing, C. Chen, Y. Zhao, G. Jia, T. Wang, H. Yuan, C. Ye, F. Zhao, Z. Chai, C. Zhu, X. Fang, B. Ma, L. Wan, Acute toxicological effects of copper nanoparticles in vivo, Toxicol. Lett. 163 (2) (2006) 109–120.
[142] D.B. Warheit, T.R. Webb, C.M. Sayes, V.L. Colvin, K.L. Reed, Pulmonary instillation studies with nanoscale TiO2 rods and dots in rats: toxicity is not dependent upon particle size and surface area, Toxicol. Sci. 91 (1) (2006) 227–236.
[143] S.D. Roy, K.C. Das, S.S. Dhar, Conventional to green synthesis of magnetic iron oxide nanoparticles; its application as catalyst, photocatalyst and toxicity: A short review, Inorg. Chem. Commun. 134 (2021), 109050.
[144] M. Arruebo, R. Fernández-Pacheco, M.R. Ibarra, J. Santamaría, Magnetic nanoparticles for drug delivery, Nano Today 2 (3) (2007) 22–32.
[145] J. Hou, Y. Wu, X. Li, B. Wei, S. Li, X. Wang, Toxic effects of different types of zinc oxide nanoparticles on algae, plants, invertebrates, vertebrates and microorganisms, Chemosphere 193 (2018) 852–860.
[146] S.J. Soenen, M. De Cuyper, Cellular toxicity of inorganic nanoparticles: Common aspects and guidelines for improved nanotoxicity evaluation, Nano Today 6 (5) (2011) 446–465.
[147] S. Yoffe, T. Leshuk, P. Everett, F. Gu, Superparamagnetic iron oxide nanoparticles (SPIONs): synthesis and surface modification techniques for use with MRI and other biomedical applications, Curr. Pharm. Des. 19 (3) (2013) 493–509.
[148] M. Mahmoudi, A. Simchi, A.S. Milani, P. Stroeve, Cell toxicity of superparamagnetic iron oxide nanoparticles, J. Colloid Interface Sci. 336 (2) (2009) 510–518.
[149] S. Bhattacharjee, L.H. de Haan, N.M. Evers, X. Jiang, A.T. Marcelis, H. Zuilhof, I. M. Rietjens, G.M. Alink, Role of surface charge and oxidative stress in cytotoxicity of organic monolayer-coated silicon nanoparticles towards macrophage NR8383 cells, Part Fibre Toxicol. 7 (2010) 25.
[150] N.M. Schaeublin, L.K. Braydich-Stolle, A.M. Schrand, J.M. Miller, J. Hutchison, J. J. Schlager, S.M. Hussain, Surface charge of gold nanoparticles mediates mechanism of toxicity, Nanoscale 3 (2) (2011) 410–420.
[151] P.R. Leroueil, S.A. Berry, K. Duthie, G. Han, V.M. Rotello, D.Q. McNerny, Jr Baker JR, B.G. Orr, M.M. Holl, Wide Varieties of Cationic Nanoparticles Induce Defects in Supported Lipid Bilayers, Nano Lett. 8 (2) (2008) 420–424.
[152] C. Chen, J. Ge, Y. Gao, L. Chen, J. Cui, J. Zeng, M. Gao, Ultrasmall superparamagnetic iron oxide nanoparticles: A next generation contrast agent for magnetic resonance imaging, WIREs Nanomed. Nanobiotechnol. 14 (1) (2022), e1740.
[153] M.O. Besenhard, L. Panariello, C. Kiefer, A.P. LaGrow, L. Storozhuk, F. Perton, S. Begin, D. Mertz, N. Thanh, A. Gavriilidis, Small iron oxide nanoparticles as MRI T 1 contrast agent: scalable inexpensive water-based synthesis using a flow reactor, Nanoscale 13 (19) (2021) 8795–8805.
[154] T.-Y. Choi, T.I. Choi, Y.R. Lee, S.K. Choe, C.H. Kim, Zebrafish as an animal model for biomedical research, Exp. Mol. Med. 53 (3) (2021) 310–317.
[155] R.J. Seeley, O.A. MacDougald, Mice as experimental models for human physiology: when several degrees in housing temperature matter, Nat. Metab. 3 (4) (2021) 443–445.
[156] Q. Ran, Y. Xiang, Y. Liu, L. Xiang, F. Li, X. Deng, Y. Xiao, L. Chen, L. Chen, Z. Li, Eryptosis Indices as a Novel Predictive Parameter for Biocompatibility of Fe3O4 Magnetic Nanoparticles on Erythrocytes, Sci. Rep. 5 (2015) 16209.
[157] X. Zhu, S. Tian, Z. Cai, Toxicity assessment of iron oxide nanoparticles in zebrafish (Danio rerio) early life stages, PLoS One 7 (9) (2012), e46286.
[158] S. Shukla, A. Jadaun, V. Arora, R.K. Sinha, N. Biyani, V.K. Jain, In vitro toxicity assessment of chitosan oligosaccharide coated iron oxide nanoparticles, Toxicol. Rep. 2 (2015) 27–39.
[159] M. Shevtsov, B. Nikolaev, Y. Marchenko, L. Yakovleva, N. Skvortsov, A. Mazur, P. Tolstoy, V. Ryzhov, G. Multhoff, Targeting experimental orthotopic glioblastoma with chitosan-based superparamagnetic iron oxide nanoparticles (CS-DX-SPIONs), Int J. Nanomed. 13 (2018) 1471–1482.
[160] C. Caro, D. Egea-Benavente, R. Polvillo, J.L. Royo, M. Pernia Leal, M.L. García-Martín, Comprehensive Toxicity Assessment of PEGylated Magnetic Nanoparticles for in vivo applications, Colloids Surf. B: Biointerfaces 177 (2019) 253–259.
[161] L. Wang, K.G. Neoh, E.T. Kang, B. Shuter, S.C. Wang, Superparamagnetic Hyperbranched Polyglycerol-Grafted Fe3O4 Nanoparticles as a Novel Magnetic Resonance Imaging Contrast Agent: An In Vitro Assessment, Adv. Funct. Mater. 19 (16) (2009) 2615–2622.
[162] S. Jahan, Y.B. Alias, A.F.B. Abu Bakar, I.B. Yusoff, Ionic release behavior of polymer-coated and uncoated metal nanoparticles (MNPs) in various conditions: effects of particle shape, size, and natural media reactivity, Colloid Polym. Sci. 295 (10) (2017) 1961–1971.
[163] K.R. Di Bona, Y. Xu, M. Gray, D. Fair, H. Hayles, L. Milad, A. Montes, J. Sherwood, Y. Bao, J.F. Rasco, Short- and Long-Term Effects of Prenatal Exposure to Iron Oxide Nanoparticles: Influence of Surface Charge and Dose on Developmental and Reproductive Toxicity, Int J. Mol. Sci. 16 (12) (2015) 30251–30268.
[164] J. Baumann, J. Köser, D. Arndt, J. Filser, The coating makes the difference: acute effects of iron oxide nanoparticles on Daphnia magna, Sci. Total Environ. 484 (2014) 176–184.
[165] E.R. de Freitas, P.R. Soares, P. Santos Rde, R.L. dos Santos, J.R. da Silva, E. P. Porfirio, S.N. Báo, E.C. Lima, P.C. Morais, L.A. Guillo, In vitro biological activities of anionic gamma-Fe2O3 nanoparticles on human melanoma cells, J. Nanosci. Nanotechnol. 8 (5) (2008) 2385–2391.
[166] A. Rafiee, M.H. Alimohammadian, T. Gazori, F. Riazi-rad, S.M.R. Fatemi, A. Parizadeh, I. Haririan, M. Havaskary, Comparison of chitosan, alginate and chitosan/alginate nanoparticles with respect to their size, stability, toxicity and transfection, Asian Pac. J. Trop. Dis. 4 (5) (2014) 372–377.
[167] I. Gehrke, A. Geiser, A. Somborn-Schulz, Innovations in nanotechnology for water treatment, Nanotechnol., Sci. Appl. 8 (2015) 1–17.
[168] Wei Wu, Zhaohui Wu, Taekyung Yu, Changzhong Jiang, Woo-Sik Kim, Recent progress on magnetic iron oxide nanoparticles: synthesis, surface functional strategies and biomedical applications, Science and Technology of Advanced Materials (2015), https://doi.org/10.1088/1468-6996/16/2/023501.